

Balancing Statistical and Computational Precision: A General Theory and Applications to Sparse Regression

Mahsa Taheri, Néhémy Lim, and Johannes Lederer

Abstract—Modern technologies are generating ever-increasing amounts of data. Making use of these data requires methods that are both statistically sound and computationally efficient. Typically, the statistical and computational aspects are treated separately. In this paper, we propose an approach to entangle these two aspects in the context of regularized estimation. Applying our approach to sparse and group-sparse regression, we show that it can improve on standard pipelines both statistically and computationally.

Index Terms—Group-feature selection, high-dimensional regression, oracle inequalities.

I. INTRODUCTION

Contemporary data sets are often large and high-dimensional: they contain many parameters and samples, and the number of parameters rivals or even exceeds the number of samples. On the other hand, one can often assume that the data generating model is sparse or group sparse, that is, that only a small number of parameters or a small number of groups of parameters, respectively, are relevant. A standard objective in the analysis of large and high-dimensional data is the selection of these relevant parameters or groups of relevant parameters in a computationally feasible and mathematically reliable way. We call these objectives feature selection and group-feature selection, respectively.

Standard approaches for these objectives such as the lasso [1] and the group lasso [2, 3] are equipped with abundant statistical theories [4, 5, 6]. But these theories concern minimizers of objective functions that can be optimized only approximately in practice, and it is unclear how replacing the true minimizers with computational surrogates impacts the theories. Moreover, these theories often assume that the tuning parameters take specific values that are not necessarily known in practice. We are, therefore, interested in interlacing statistical aspects, computational aspects, and tuning parameter calibration.

In this paper, we interweave optimization theory and statistical theory via oracle inequalities. This approach allows us to

develop a general algorithm and corresponding statistical theories that account for the optimization aspect and for tuning-parameter calibration. In effect, we obtain lasso- and group-lasso-type methods that are faster and more accurate than competing methods and equipped with more comprehensive statistical guarantees.

A. Related Work and Contributions

One basis of our paper are so-called oracle inequalities. Oracle inequalities are bounds for the statistical errors of estimators [4]. Usually, these bounds hold “with high-probability,” that is, they hold on an event that is increasing with the sample size. Two main problems with standard oracle inequalities are that they (i) assume tuning parameters that depend on unknown parameters (such as the distribution of the noise) and (ii) do not account for any optimization aspects.

A solution for the first problem has been proposed in Chichignoud et al. [7]. Indeed, the AV method in Chichignoud et al. [7, Algorithm 1] provides tuning-parameter calibration that leads to—in some sense optimal—oracle inequalities [7, Theorem 3]. The original AV method was designed for lasso in linear regression; in the meantime, extensions to logistic regression, graphical models, personalized medicine, and refitted estimation in linear regression have been established [8, 9, 10, 11]. However, these theories still assume that the estimators are computed perfectly, that is, they still do not solve the second problem mentioned above.

In Section II, we extend the above works to solve both mentioned problems. In other words, we establish a general algorithm (Algorithm 1) that satisfies oracle inequalities (Theorem 1) accounting both for tuning-parameter calibration and for potentially inaccurate optimization.

In Section III, we exemplify our general approach in linear regression and logistic regression. We find that the approach not only leads to favorable oracle inequalities but also makes lasso- and group-lasso-type estimation and feature selection faster and more accurate.

B. Notation

For any set \mathcal{A} and any vector $\beta \in \mathbb{R}^p$, we denote by $\beta_{\mathcal{A}} \in \mathbb{R}^p$ the vector that equals β on the coordinates in \mathcal{A} and is zero on the coordinates in the complement of \mathcal{A} , and for any given matrix $X \in \mathbb{R}^{n \times p}$, we denote by $X_{\mathcal{A}} \in \mathbb{R}^{n \times |\mathcal{A}|}$ the submatrix of X with column indices in \mathcal{A} . For any vector $\beta \in \mathbb{R}^p$, we define the support set of β as $\text{supp}(\beta) := \{j \in \{1, \dots, p\} :$

arXiv:1609.07195v3 [stat.ME] 14 Sep 2022

(Corresponding author: Mahsa Taheri)

M. Taheri and J. Lederer are with the Department of Mathematics, Ruhr-University Bochum, 44801 Bochum, Germany (e-mail: mahsa.taheri@rub.de; johannes.lederer@rub.de).

N. Lim is with Business and Decision Benelux, 1200 Woluwe-Saint-Lambert, Belgium (email: nehemy.lim@businessdecision.be).

$\beta_j \neq 0\}$. We denote the ℓ_q -norm for vectors by $\|\cdot\|_q$ for $q \in [1, \infty]$. For any matrix $Q \in \mathbb{R}^{n \times p}$, we define the matrix norm induced by the ℓ_q -norm, denoted by $\|\cdot\|_q$ as follows:

$$\|Q\|_q := \sup_{\mathbf{x} \neq \mathbf{0}_p} \frac{\|Q\mathbf{x}\|_q}{\|\mathbf{x}\|_q}.$$

The minimal eigenvalue of a square matrix is denoted by $\Omega_{\min}(\cdot)$.

To disentangle theory and practice, we use bars $\bar{\cdot}$ to refer to theoretical estimators (for example, one cannot compute an exact lasso solution in finite time) and tildes $\tilde{\cdot}$ to practical surrogates (for example, one can approximate a lasso solution within any non-zero tolerance). To avoid heavy notation, some notation can have different meanings depending on whether we treat linear or logistic regression.

II. METHODOLOGY

In this section, we state the statistical framework and introduce our estimation approach along with guarantees for it.

A. Motivation

Consider a standard linear regression model

$$\mathbf{y} = X\boldsymbol{\beta}^* + \mathbf{u}$$

with $\mathbf{y} \in \mathbb{R}^n$, $X \in \mathbb{R}^{n \times p}$, $\boldsymbol{\beta}^* \in \mathbb{R}^p$, and $\mathbf{u} \in \mathbb{R}^n$. In genomics, for example, \mathbf{y} could contain the levels of a biomarker, X the counts of different SNPs, $\boldsymbol{\beta}^*$ the statistical associations between the SNPs and the biomarker, and \mathbf{u} the measurement errors, batch effects, non-linearities, etc. The number of SNPs in typical studies is in the millions, while the number of study subjects is much smaller: $p \gg n$ [12]. We call such settings *high-dimensional*.

In high-dimensional regression, classical estimators such as the least-squares estimator are prone to overfitting. More appropriate are regularized approaches such as the lasso [1]

$$\bar{\boldsymbol{\beta}}^r \in \operatorname{argmin}_{\boldsymbol{\beta} \in \mathbb{R}^p} \left\{ \frac{1}{2} \|\mathbf{y} - X\boldsymbol{\beta}\|_2^2 + r \|\boldsymbol{\beta}\|_1 \right\},$$

which is a family of ℓ_1 -regularized least-squares estimators indexed by a tuning parameter $r \in [0, \infty)$. A feature of the lasso family is that it can provide small models: $\#\{(\bar{\boldsymbol{\beta}}^r)_j \neq 0\} \ll p$. In genomics, for example, this means that the number of SNPs the estimator deems relevant is small, which can facilitate interpretation and further processing. In general, we call the identification of the most relevant predictors *feature selection*.

But regularized approaches such as the lasso spawn three objectives:

1) Selecting the tuning parameter r

Large tuning parameters can prevent overfitting, but they also introduce a large bias. A selection scheme must, therefore, balance these two aspects.

2) Computing the estimators

The lasso's objective function, for example, is convex and "almost smooth" but rarely has a minimizer in closed-form. More generally, regularized estimators can usually be

computed only approximately with descent algorithms such as proximal gradient or coordinate descent. But these descent algorithms involve another tuning parameter, namely, the number of descent steps. Picking a large number of steps ensures that the outputs approximate the actual minimizer well, but this also renders computations slow or even infeasible. So a good strategy for calibrating the number of descent steps is needed.

3) Choosing cutoffs for feature selection

Regularized estimators often undergo further treatment such as thresholding. Thresholding can remove numerical and statistical artifacts and, therefore, reduce the number of false positives. But thresholding involves yet another tuning parameter, namely, the cutoff. Large cutoffs remove false positives effectively but can also lead to a large number of false negatives. Hence, a sound way to calibrate the cutoff is also in order.

In the context of the lasso, each of the three objectives individually is understood at least to some extent: for objective 1, see [7, 13], for example; for objective 2, see [14, 15], for example; for objective 3, see [7, 11], for example. In this paper, however, we address all three objectives simultaneously, leading to more comprehensive guarantees in theory and to faster and better performances in practice.

B. Statistical Framework

We now move from the lasso to a more general statistical framework. Our goal is to estimate an unknown target $\boldsymbol{\beta}^* \in \mathcal{B}$ in a non-empty set \mathcal{B} . We consider a family of "theoretical" estimators $\mathcal{F}_{\mathcal{R}} := \{\bar{\boldsymbol{\beta}}^r : r \in \mathcal{R}\}$ indexed by a non-empty set of tuning parameters $\mathcal{R} \subset \mathbb{R}$ and a corresponding family of "practical" estimators $\tilde{\mathcal{F}}_{\mathcal{R}} := \{\tilde{\boldsymbol{\beta}}^r : r \in \mathcal{R}\}$. The rationale beyond this distinction is that statistical theory in high dimensions is typically formulated for infeasible estimators (such as the lasso) but that these infeasible estimators can be approximated well by practical algorithms (such as proximal gradient descent).

Our starting point is the statistical and computational theory that is typically available in high dimensions.

Assumption 1 (Theory basis): Consider a function $d : \mathcal{B} \times \mathcal{B} \rightarrow [0, \infty)$ that is symmetric and satisfies the triangle inequality, and consider functions $f, g : \mathcal{R} \rightarrow [0, \infty)$ that are increasing. Given an oracle parameter $\boldsymbol{\beta}^* \in \mathcal{B}$ and an oracle tuning parameter $r^* \in \mathcal{R}$, we assume the "statistical" bound

$$d(\bar{\boldsymbol{\beta}}^r, \boldsymbol{\beta}^*) \leq f(r) \quad \forall r \geq r^* \quad (1)$$

and the "computational" bound

$$d(\tilde{\boldsymbol{\beta}}^r, \bar{\boldsymbol{\beta}}^r) \leq g(r) \quad \forall r \geq r^*. \quad (2)$$

Broadly speaking, Assumption (1) ensures that there is a theoretical guarantee for large enough tuning parameters. Such guarantees are abundant in high-dimensional statistics [4].

Assumption (2) ensures that the theoretical estimators can be approximated well. In other words, Assumption (2) specifies what we mean by "practical estimators:" these are estimators that are close to their theoretical counterparts in terms

of the distance d . Such guarantees, unfortunately, are rare in the literature. However, in the applications in Section III, we relate these guarantees to guarantees in terms of the objective function, which can then be readily checked by the algorithms. It would also be very interesting to relate the d -guarantees to criteria other than the value in objective function, such as run times of the algorithm, in future work. In any case, note that different algorithms might lead to different bounds $g(r)$.

The function d is the distance function. Typical examples in linear regression are $d : (\beta, \beta^*) \mapsto \|\beta - \beta^*\|_q$ for a $q \in [1, \infty]$. The oracle parameter β^* is the “true” parameter or any surrogate of it. A generic example in linear regression is the true regression vector.

The oracle tuning parameter r^* can be any tuning parameter in \mathcal{R} that makes Assumption 1 go through. This seems quite abstract here in the general setup but will clarify in the specific applications in the later sections. In linear regression with the lasso, for example, it is straightforward to identify $r^* = 2\|X^\top \mathbf{u}\|_\infty$ (or the closest surrogate of it in \mathcal{R}) as a natural choice—we will come back to this on Page 5. Important here is that r^* does not need to be known in practice.

C. Proposed Method and Theoretical Results

We now propose a pipeline that deals with our Objectives 1.–3. stated earlier. Given a family of theoretical estimators $\mathcal{F}_{\mathcal{R}}$ and a corresponding family of practical estimators $\tilde{\mathcal{F}}_{\mathcal{R}}$, a distance function d , and functions f and g as specified in Assumption 1, our first goal is selecting a practical estimator $\tilde{\beta}^{\hat{r}}$ that is guaranteed to have a small distance $d(\tilde{\beta}^{\hat{r}}, \beta^*)$. The best possible guarantee in the sense of Assumption 1 is

$$d(\tilde{\beta}^{r^*}, \beta^*) \leq f(r^*) + g(r^*).$$

But since neither β^* nor r^* are known in practice, we have to make a data-driven selection of r .

Our proposal for this selection is summarized in Algorithm 1. The general idea is as follows: Estimators that correspond to tuning parameters that are sufficiently large are “steady,” while estimators that correspond to tuning parameters that are too small behave “erratically” in high-dimensional settings (think of unregularized estimators in the limit). The algorithm detects this transition by comparing differences between estimators.

Algorithm 1 shares its general idea with the AV approach [7, Algorithm 1] but generalizes that approach in two aspects: it generalizes it from the lasso to our broad statistical framework, and it includes the computational discrepancies g . These generalizations, however, make the proofs considerably more difficult. The main technical challenge is that we can no longer use the theoretical properties of minima of an objective function (KKT conditions, for example). We overcome this challenge with careful comparisons of the theoretical and practical estimators.

On a technical level, for the while-loop to make sense and to ensure that the algorithm converges, we assume here and in the following that the set of tuning parameters \mathcal{R} is finite—but,

Algorithm 1: general approach

Inputs : \mathcal{R}, d, f, g

Outputs: $\hat{r} \in \mathcal{R}, \tilde{\beta}^{\hat{r}} \in \mathcal{B}$

```

1 Initialize tuning parameter:  $\tilde{r} \leftarrow \max\{r \in \mathcal{R}\}$ ;
2 Compute  $\tilde{\beta}^{\tilde{r}}$ ;
3 while  $\tilde{r} \neq \min\{r \in \mathcal{R}\}$  and  $\nexists r \in \mathcal{R} \setminus (-\infty, \tilde{r}]$  :
     $d(\tilde{\beta}^{\tilde{r}}, \tilde{\beta}^{\tilde{r}}) > f(r) + g(r) + f(\tilde{r}) + g(\tilde{r})$  do
4     Update outputs:  $\hat{r} \leftarrow \tilde{r}$ ;  $\tilde{\beta}^{\hat{r}} \leftarrow \tilde{\beta}^{\tilde{r}}$ ;
5     Go to next tuning parameter:
       $\tilde{r} \leftarrow \max\{r \in \mathcal{R} \setminus [\tilde{r}, \infty)\}$ ;
6     Compute  $\tilde{\beta}^{\tilde{r}}$ ;
7 end
```

importantly, it can be arbitrarily large. (We will show later that the specific construction of this set is of minor importance.)

We find the following guarantee for Algorithm 1.

Theorem 1 (Guarantee for \hat{r} and $\tilde{\beta}^{\hat{r}}$): Under Assumption 1, the outputs \hat{r} and $\tilde{\beta}^{\hat{r}}$ of Algorithm 1 satisfy

$$\hat{r} \leq r^*, \quad (3)$$

$$d(\tilde{\beta}^{\hat{r}}, \beta^*) \leq 3f(r^*) + 3g(r^*), \quad (4)$$

and

$$\mathbb{E}[d(\tilde{\beta}^{\hat{r}}, \beta^*)] \leq 3\mathbb{E}f(r^*) + 3\mathbb{E}g(r^*). \quad (5)$$

The proof of Theorem 1 is deferred to Appendix A. There, we also state a generalization that allows for deviations from \hat{r} (see Lemma 10).

Inequality (3) states that the estimated tuning parameter is bounded by the optimal tuning parameter; this result will be useful in thresholding small coefficients. Inequality (4) states that the selected estimator reaches the best possible bound up to the constant factor 3. Inequality (5) states the same in expectation.

Note that Inequalities (3) and (4) are entirely “deterministic:” they always hold under the stated assumptions. All probabilistic aspects are summarized in the typically random quantity r^* —see the following sections with the examples. The feature of being “deterministic” keeps the bounds very general and allows us to derive Inequality (5) in a rather trivial fashion.

The oracle quantities β^* and r^* are usually unknown. But, quite strikingly, our method is guaranteed to be essentially optimal even without knowing these quantities. (Yet, not knowing r^* , we cannot derive confidence intervals from the theorem.) On the other hand, the functions d , f , and g need to be specified beforehand. We exemplify the pipeline for common choices of these functions in the following section. The choice of the set of tuning parameters \mathcal{R} is usually secondary: in practice, one can just choose an ad-hoc, “standard” grid over the relevant values. This is not completely obvious but follows from a detailed look at our theories and the typical way the practical estimators are computed: In our theoretical guarantees, the set \mathcal{R} only appears through r^* , that is, the finer the grid \mathcal{R} , the better its best representative $r^* \in \mathcal{R}$.

In other words, the finer the grid, the better the guarantees. In practice, on the other hand, fine grids also require the computation of many estimators. But since the estimators are usually computed with warmstarts, additional estimators are typically fast to compute. Moreover, given the structure of the algorithm, estimators with $r \leq \hat{r}$ do not need to be computed altogether. We find in the numerical experiments described in the following section that “standard” tuning parameter sets such as logarithmically spaced grids with 100 elements give excellent performance. Also, additional simulations illustrate the limited influence of the specific choice of the tuning parameter set (see Appendix B-C). An open question at this point, however, is how to choose \mathcal{R} optimally.

The above bounds parallel those in [7, Theorem 3]. But besides generalizing the bounds to our framework, Theorem 1 contains another, more subtle, improvement: while Chichignoud et al. [7, Theorem 3] set the oracle tuning parameter to quantiles of the effective noise $2\|X^\top \mathbf{u}\|_\infty$, our theorem here also allows for setting $r^* = 2\|X^\top \mathbf{u}\|_\infty$ directly. The latter choice seems more natural and avoids the introduction of quantiles and corresponding levels. Moreover, it allows us to state bounds in expectation.

The above theories are not only useful for the selection of the tuning parameter r , but they also motivate approaches to our Objectives 2. (descent steps) and 3. (cutoff). More precisely, the proposed algorithm and its theoretical guarantees motivate a holistic approach that covers all three Objectives 1.–3. simultaneously. Increasing the number of descent steps improves the approximations, that is, decreases g , but also adds a computational burden. Bounds (4) and (5) motivate to calibrate the number of steps such that $g = f$: this choice (i) ensures that the practical estimators are equipped with the same statistical bounds as the theoretical estimators up to a factor of two and, as we will see in the example section, (ii) leads to a large increase in computational speed in comparison to pipelines that attempt to descend “until convergence”.

The bounds (4) and (5) also motivate a cutoff for feature selection. Say $\mathcal{B} \subset \mathbb{R}^p$. Feature selection, or more generally group-feature selection consists of estimating the support set $\mathcal{S} := \text{supp}(\boldsymbol{\beta}^*) := \{j \in \{1, \dots, k\} : \beta_{G^j}^* \neq \mathbf{0}_{p_j}\}$, where G^1, \dots, G^k is a partition of $\{1, \dots, p\}$ and p_j is the size of group G^j . Typical measures of estimation accuracy d are the metrics induced by the $\ell_{q,\infty}$ -norm with $q \in [1, \infty]$ [16]:

$$d(\boldsymbol{\beta}, \boldsymbol{\beta}') := \|\boldsymbol{\beta} - \boldsymbol{\beta}'\|_{q,\infty} := \max_{j \in \{1, \dots, k\}} \left(\sum_{l \in G^j} |\beta_l - \beta'_l|^q \right)^{1/q} \quad \forall \boldsymbol{\beta}, \boldsymbol{\beta}' \in \mathbb{R}^p. \quad (6)$$

We then propose feature selection with the thresholding scheme

$$\hat{\mathcal{S}} := \{j \in \{1, \dots, k\} : \|\tilde{\boldsymbol{\beta}}_{G^j}^{\hat{r}}\|_q > 3f(\hat{r}) + 3g(\hat{r})\}, \quad (7)$$

where \hat{r} and $\tilde{\boldsymbol{\beta}}^{\hat{r}}$ are the outputs of Algorithm 1. And we can find the following guarantee for $\hat{\mathcal{S}}$.

Lemma 2 (Group-feature selection): Assume the beta-min condition

$$\min_{j \in \mathcal{S}} \|\boldsymbol{\beta}_{G^j}^*\|_q > 6f(r^*) + 6g(r^*).$$

Then, it holds that

$$\hat{\mathcal{S}} = \mathcal{S}.$$

Hence, as long as the ℓ_q -norms of the non-zero groups of the true vector are not too small, one can safely threshold each group of $\tilde{\boldsymbol{\beta}}^{\hat{r}}$ with the cutoff $3f(\hat{r}) + 3g(\hat{r})$ without increasing the number of false negatives.

Note that Lemma 2 as well as Theorem 1 are stochastic: the randomness of the data is reflected in the oracle tuning parameter r^* .

III. EXAMPLES

In this section, we exemplify our general approach. We consider $\mathcal{B} := \mathbb{R}^p$ and a measure of accuracy d that is induced by a norm: $d(\boldsymbol{\beta}, \boldsymbol{\beta}') := \|\boldsymbol{\beta} - \boldsymbol{\beta}'\|$. The theoretical estimators are defined by

$$\bar{\boldsymbol{\beta}}^r \in \underset{\boldsymbol{\beta} \in \mathbb{R}^p}{\text{argmin}} \ell(\boldsymbol{\beta}, r)$$

for $r \in \mathcal{R} \subset [0, \infty)$ and $\ell(\boldsymbol{\beta}, r) := L(\boldsymbol{\beta}) + r\|\boldsymbol{\beta}\|^\dagger$ with a convex and differentiable function $L : \mathbb{R}^p \rightarrow [0, \infty)$. Specifically, we take L as the least-squares loss (Section III-A) and the logistic loss (Section III-B). Our conditions on the regularizer—besides it being a norm is: 1. decomposability with respect to the support $\mathcal{S} = \text{supp}(\boldsymbol{\beta}^*)$ of the target $\boldsymbol{\beta}^*$, that is, $\|\boldsymbol{\beta}\|^\dagger = \|\boldsymbol{\beta}_{\mathcal{S}}\|^\dagger + \|\boldsymbol{\beta}_{\mathcal{S}^c}\|^\dagger$ for all $\boldsymbol{\beta} \in \mathbb{R}^p$, which holds for many standard regularizers, for example, see [17, Section 2.2] and [18, Section 3.2] and 2. the regularizer is the dual norm of $\|\cdot\|$ (induced norm in the measure of accuracy d).

A. Linear Regression

Here, we specify our approach to regularized linear regression. In Section III-A1, we provide sufficient conditions for Assumption (1) and Assumption (2) (see Lemma 3 and Lemma 4, respectively), and we exemplify the results by considering group-feature selection with the group lasso. In Section III-A2, we specify the implementation for group-feature selection (see Algorithm 2), and in Section III-A3, we demonstrate the empirical efficiency of our approach both on simulated and real data.

1) *Method:* We can apply our general scheme in Algorithm 1 to the linear regression model

$$\mathbf{y} = X\boldsymbol{\beta}^* + \mathbf{u},$$

where $\mathbf{y} \in \mathbb{R}^n$ is the outcome, $X \in \mathbb{R}^{n \times p}$ the design matrix, $\boldsymbol{\beta}^* \in \mathbb{R}^p =: \mathcal{B}$ the regression vector with support $\mathcal{S} = \text{supp}(\boldsymbol{\beta}^*) \subset \{1, \dots, p\}$, and $\mathbf{u} \in \mathbb{R}^n$ the random noise. To estimate $\boldsymbol{\beta}^*$, we consider the objective function

$$\ell(\boldsymbol{\beta}, r) := L(\boldsymbol{\beta}) + r\|\boldsymbol{\beta}\|^\dagger, \quad (8)$$

where $\boldsymbol{\beta} \in \mathbb{R}^p$, $r \in [0, \infty) =: \mathcal{R}$, and $L(\boldsymbol{\beta}) := \|\mathbf{y} - X\boldsymbol{\beta}\|_2^2/2$. We then propose to use the estimators $\mathcal{F}_{\mathcal{R}} = \{\bar{\boldsymbol{\beta}}^r : r \in \mathcal{R}\}$ with

$$\bar{\boldsymbol{\beta}}^r \in \underset{\boldsymbol{\beta} \in \mathbb{R}^p}{\text{argmin}} \ell(\boldsymbol{\beta}, r). \quad (9)$$

A sufficient condition for satisfying the statistical bound in Assumption (1) for the estimators in Display (9) is as follows:

Lemma 3 (f in regularized linear regression): Assume there is a constant $c \in (0, \infty)$ such that

$$\|\boldsymbol{\nu}\| \leq \frac{\|X^\top X \boldsymbol{\nu}\|}{nc} \quad \forall \boldsymbol{\nu} \in \mathbb{R}^p : \|\boldsymbol{\nu}_{S^c}\|^\dagger \leq 3\|\boldsymbol{\nu}_S\|^\dagger.$$

Then, $\mathcal{F}_{\mathcal{R}}$ satisfies

$$\|\boldsymbol{\beta}^* - \tilde{\boldsymbol{\beta}}^r\| \leq f(r) \quad \forall r \geq r^*$$

for $f(r) := 3r/(2nc)$ and $r^* := 2\|X^\top \mathbf{u}\|$.

The condition in the upper display of the lemma is a variant of the classical compatibility condition [19, 20]. If $\|\cdot\| \equiv \|\cdot\|_\infty$, for example, it coincides with the ℓ_∞ -restricted eigenvalue condition formulated in [7, Equation (7)]; in this sense, Lemma 3 is a generalization of their Lemma 5. We defer the proof of Lemma 3 to Appendix A.

The lemma also clarifies the choice of the oracle tuning parameter r^* in linear regression. Recall that in the abstract setup of Section II, the oracle tuning parameter could be any tuning parameter that makes the assumptions go through; here, we identify $r^* := 2\|X^\top \mathbf{u}\|$ as a valid choice in linear regression. In the lasso case, where $\|\cdot\| \equiv \|\cdot\|_\infty$, the value of the oracle tuning parameter coincides with the usual value in the literature—see, for example, [21, Pages 1–2], Lederer et al. [22, Page 9], and Lederer [4, Page 112]. Thus, in line with that standard literature, we can interpret r^* as the “best” tuning parameter in the sense that it is the smallest tuning parameter that controls the effective noise [23, Section 4].

A sufficient condition for satisfying the computational bound in Assumption (2) for estimators in Equation (9) is as follows:

Lemma 4 (g in regularized regression): For given $b \in [0, \infty)$, assume there is a constant $z \in (0, \infty)$ such that

$$L(\boldsymbol{\beta} + \boldsymbol{\nu}) - L(\boldsymbol{\beta}) - \langle \nabla L(\boldsymbol{\beta}), \boldsymbol{\nu} \rangle \geq zn\|\boldsymbol{\nu}\|^\dagger{}^2$$

for all $\boldsymbol{\beta} \in \mathbb{R}^p$ and $\boldsymbol{\nu} \in \mathbb{R}^p$ that satisfy $\|\boldsymbol{\nu}_{S^c}\|^\dagger \leq 3\|\boldsymbol{\nu}_S\|^\dagger + 4\|\tilde{\boldsymbol{\beta}}_{S^c}^r\|^\dagger + b/r$. Assume also that $\|\cdot\| \leq \|\cdot\|^\dagger$. Then, we have

$$\|\tilde{\boldsymbol{\beta}}^r - \tilde{\boldsymbol{\beta}}\| \leq g(r) \quad \forall r \in [r^*, \infty)$$

for $g(r) := \sqrt{b/(zn)} + r/(zn)$ and every $\tilde{\boldsymbol{\beta}} \in \mathbb{R}^p$ with $\ell(\tilde{\boldsymbol{\beta}}, 2r) \leq \ell(\tilde{\boldsymbol{\beta}}^r, 2r) + b$.

Above lemma gives a tool to check whether the “computational bound” is reached by using the objective’s value: once $\ell(\tilde{\boldsymbol{\beta}}, 2r) \leq \ell(\tilde{\boldsymbol{\beta}}^r, 2r) + b$ is verified, then, we can make sure that $\|\tilde{\boldsymbol{\beta}}^r - \tilde{\boldsymbol{\beta}}\| \leq g(r)$ is verified as well for $g(r) := \sqrt{b/(zn)} + r/(zn)$. The result is formulated for general convex and differentiable loss functions to make it useful also for the case of logistic regression in the next section. The condition in the upper display of the lemma is a slightly stronger version of restricted strong convexity [24, Pages 291ff], [6, Pages 277ff] (see Section B-A for details).

Now, plugging Lemma 3 and Lemma 4 into Theorem 1 yields the following result.

Corollary 5 (Estimation in regularized linear regression): Suppose that the conditions of Lemma 3 are met and $g = f$. Then, the outputs of Algorithm 1 satisfy

$$\hat{r} \leq r^*,$$

$$d(\tilde{\boldsymbol{\beta}}^{\hat{r}}, \boldsymbol{\beta}^*) \leq 9r^*/(nc),$$

and

$$\mathbb{E}[d(\tilde{\boldsymbol{\beta}}^{\hat{r}}, \boldsymbol{\beta}^*)] \leq \mathbb{E}[9r^*/(nc)].$$

This equips the proposed algorithm with guarantees for its estimation error in linear regression models.

Besides estimation, our approach can also be applied to feature selection. Specifically suited base estimators for feature selection are sparsity-inducing methods, such as the group lasso:

$$\tilde{\boldsymbol{\beta}}^r \in \operatorname{argmin}_{\boldsymbol{\beta} \in \mathbb{R}^p} \left\{ \frac{1}{2} \|\mathbf{y} - X\boldsymbol{\beta}\|_2^2 + r \sum_{j=1}^k \sqrt{p_j} \|\boldsymbol{\beta}_{G^j}\|_2 \right\},$$

which corresponds in our framework to the distance

$$d(\boldsymbol{\beta}, \boldsymbol{\beta}') := \max_{j \in \{1, \dots, k\}} \|\boldsymbol{\beta}_{G^j} - \boldsymbol{\beta}'_{G^j}\|_2 / \sqrt{p_j} \quad \forall \boldsymbol{\beta}, \boldsymbol{\beta}' \in \mathbb{R}^p.$$

An estimate of the support with our thresholding scheme is

$$\hat{\mathcal{S}} := \{j \in \{1, \dots, k\} : \|\tilde{\boldsymbol{\beta}}_{G^j}^{\hat{r}}\|_2 / \sqrt{p_j} > 9\hat{r}/(nc)\}, \quad (10)$$

where \hat{r} and $\tilde{\boldsymbol{\beta}}^{\hat{r}}$ are the outputs of Algorithm 1 with $f(r) := g(r) := 3r/(2nc)$. Assuming the above-mentioned compatibility condition and an equally standard beta-min condition [4, 5]

$$\min_{j \in \mathcal{S}} \|\boldsymbol{\beta}_{G^j}^*\|_2 / \sqrt{p_j} > \frac{18r^*}{nc},$$

we obtain a sharp guarantee for $\hat{\mathcal{S}}$:

Corollary 6 (Group-feature selection in regularized linear regression): Under the stated conditions, it holds that

$$\hat{\mathcal{S}} = \mathcal{S}.$$

This guarantee takes both the tuning parameter calibration and the computational tolerances of the implementations into account; in other words, Equation (10) is a theoretically justified thresholding scheme.

2) *Algorithm:* Algorithm 2 is a specification of our general scheme for group-feature selection in linear regression. Recall that bars refer to theoretical estimators, while tildes refer to computable surrogates. We call the algorithm group-FOS (group-Fast and Optimal Selection) for convenient reference. The three challenges described earlier are addressed as follows: (1) The stopping point on the tuning parameter path is determined via AV-tests [7], which contrasts estimators in terms of the distance function (line 19 of Algorithm 2). Note that here, Equation (6) is used as the distance function. (2) We use the duality gap to ensure that the computational bound is reached. For any regression vector $\tilde{\boldsymbol{\beta}}$ and any feasible dual variable $\tilde{\boldsymbol{\nu}}$, the duality gap is $\Delta(\tilde{\boldsymbol{\beta}}, \tilde{\boldsymbol{\nu}}) := \ell(\tilde{\boldsymbol{\beta}}, 2r) - D(\tilde{\boldsymbol{\nu}}, 2r)$, where $D(\tilde{\boldsymbol{\nu}}, 2r)$ is the dual function, and it is well known [25] that $\Delta(\tilde{\boldsymbol{\beta}}, \tilde{\boldsymbol{\nu}})$ is an upper bound of $\ell(\tilde{\boldsymbol{\beta}}, 2r) - \ell(\tilde{\boldsymbol{\beta}}^{2r}, 2r)$. Since $\ell(\tilde{\boldsymbol{\beta}}^{2r}, 2r) \leq \ell(\tilde{\boldsymbol{\beta}}^r, 2r)$, we conclude that $\Delta(\tilde{\boldsymbol{\beta}}, \tilde{\boldsymbol{\nu}})$ is also an upper bound of $\ell(\tilde{\boldsymbol{\beta}}, 2r) - \ell(\tilde{\boldsymbol{\beta}}^r, 2r)$. This upper bound ensures that the required precision is reached. Importantly, we do not need to solve the dual problem of the group lasso, but instead, we only require a dual point, which can be found with an explicit expression. We refer to Lemma 4 to show the connection between computational bound and

duality gap and Appendix B-B regarding the construction of feasible dual points. Setting $f(r) := g(r) := 3r/(2nc)$, which, by Lemma 4, gives the stopping criterion as $\Delta(\tilde{\beta}, \tilde{\nu}) \leq b := r^2(3z/(2c) - 1)^2/(zn)$. As the optimization algorithm, one could select proximal gradient descent [26], coordinate descent [14], or other techniques. We opted for the first one; the corresponding updates in line 14 then read for each group

$$\tilde{\beta}_{G^j} \mapsto \mathcal{T}_{r\sqrt{p_j}/m}(\tilde{\beta}_{G^j} - \frac{1}{m}X_{G^j}^\top(X\tilde{\beta} - \mathbf{y})),$$

where \mathcal{T} is the block soft-thresholding operator defined by $\mathcal{T}_t(\mathbf{a}_{G^j}) := \max(1 - t/\|\mathbf{a}_{G^j}\|_2, 0)\mathbf{a}_{G^j}$ for $j \in \{1, \dots, k\}$ and where $m \in (0, \infty)$ is the step size determined by backtracking. (3) We finally use Equation (10) for thresholding, which guarantees correct (group) feature selection (see Corollary 6).

Neglecting all the intricate details, our method is simply a roughly computed group lasso estimate with subsequent thresholding of the elements.

As initialization, we choose the all-zeros vector in \mathbb{R}^p , reflecting our assumption that many groups are inactive. Since we are limited to finitely many computations in practice, we consider finite sequences $r_1 = r_{\max} > r_2 > \dots > r_M = r_{\min} > 0$. The concrete choice follows the ones used in standard implementations [14]: we use a logarithmically spaced grid of size $M = 100$, set $r_{\max} := \max_{j \in \{1, \dots, k\}} \|X_{G^j}^\top \mathbf{y}\|_2 / \sqrt{p_j}$ to the smallest tuning parameter such that $\tilde{\beta}^* = \mathbf{0}_p$, and define $r_{\min} := r_{\max}/h$ as a fraction of r_{\max} . Standard choices for h range from 100 to 10 000. On a very high level, assuming bounded group sizes, it holds that $r_{\max}/r^* \approx \max_{j \in \{1, \dots, k\}} \|X_{G^j}^\top \mathbf{y}\|_2 / \max_{j \in \{1, \dots, k\}} \|X_{G^j}^\top \mathbf{u}\|_2 \approx n \sum_{j=1}^k \sqrt{p_j} \|\beta_{G^j}^*\|_2 / \sqrt{n} \approx \sqrt{n}$. To ensure that $r_{\min} < r^*$ on our data sets, we thus select $h := 1000$. Moreover, note that our theoretical results hold for any types of grids (also for continuous ranges of r). And because of the warm starts and the early stopping, the computational complexity of group-FOS depends only very mildly on M and r_{\min} . Finally, $c = 2$ and $z = 1$ are considered global constants. We show later that changing these constants has minor impact on our results (see Tables VIII and IX).

Computationally, the proposed method has two main advantages: First, only a part of the tuning parameter path needs to be computed, more precisely, only the part with large and moderate tuning parameters. Second, only very rough computations are required; in particular, since a large tolerance can be accepted for large tuning parameters, only very small numbers of optimization cycles (in practice, often zero to five) are required per tuning parameter.

3) *Empirical performance:* We now demonstrate the computational efficiency and the empirical accuracy of the proposed method. To obtain a comprehensive overview, we consider a variety of experiments for feature selection and group-feature selection, including biological and financial applications as well as synthetic data. group-FOS can be adapted easily to handle data without structure; we call this version FOS for convenient reference. We compare FOS to the lasso with Cross-Validation (lassoCV), which is currently the most

popular method for feature selection, and with the non-convex approaches SCAD [27] and MCP [28]; and we compare group-FOS with the group lasso with Cross-Validation (group-lassoCV). We start by synthetic data sets to verify the efficiency of FOS and group-FOS in regressions with moderately large data (up to 10 000 samples and parameters). Then, we show the scalability of FOS by analyzing a financial data set with more than 150 000 parameters. (The application to even larger regression data is currently limited by the memory restrictions in MATLAB[®]; a future C/Fortran implementation could remove this limitation). We continue by learning a biological network with a neighborhood selection scheme. Each of the corresponding regressions comprises only 500 samples and 1000 parameters, but since 1000 such regressions are needed, the computational complexity can easily render standard methods infeasible. Finally, we show the efficiency of group-FOS in classification on biological data.

All computations are conducted with MATLAB[®] and are run on an Intel Core(TM) i5-3470 CPU(3.20GHz). FOS and group-FOS are implemented using the SPAMS package [29] coded in C++, which uses the duality gap as the convergence criterion. The frequency for checking the duality gap is set to every 1 iteration in the optimization function. FOS is compared with two lassoCV implementations: First, lassoCV is implemented analogously to FOS using the SPAMS package and a 10-fold Cross-Validation with warm starts. This implementation, called lassoCV_{SPAMS} in the following, is the most appropriate one for comparisons with the FOS implementation. However, much work has gone into efficient implementations of lassoCV. Therefore, we also use the well-known glmnet package [14] and call the corresponding implementation lassoCV_{glmnet}. However, these results must be treated with reservation, because glmnet cannot be calibrated to the same convergence criterion as our implementation. More precisely, the convergence criterion in glmnet needs to be specified in terms of maximum change in the objective, which does not coincide with the criterion in our algorithm and with the convergence of the estimator itself as needed in the theory. One could also argue that comparing FOS with lassoCV_{glmnet} is not fair in any case, because glmnet exploits additional geometric properties of the lasso (such as screening rules). These additional properties could also be used in our scheme, but their implementation is deferred to future work. In any case, we demonstrate that even in its current version, FOS can outperform both lassoCV_{SPAMS} and lassoCV_{glmnet}. For SCAD and MCP, we use the SparseReg toolbox [30]. The tuning parameters that balance the fitting and penalty are set via Cross-Validation. However, SCAD and MCP each also contain a second tuning parameter that determines the shape of the penalty: for SCAD, it is set to 3.7, which minimizes the Bayes risk; for MCP, it is set to 1, the default value in the SparseReg toolbox. group-lassoCV_{SPAMS} is implemented analogously to group-FOS, using the SPAMS package and a 10-fold Cross-Validation with warm starts.

Code can be found under github.com/LedererLab.

a) *Synthetic data:* In this part, we use synthetic data to demonstrate the empirical performance of FOS and group-FOS. For FOS, data are generated from linear regression

Algorithm 2: group-feature selection in linear regression

Inputs : $\mathbf{y} \in \mathbb{R}^n$; $X \in \mathbb{R}^{n \times p}$; $r_1 = r_{\max} > r_2 > \dots > r_M > 0$
Outputs: $\tilde{\beta}^{\hat{r}} \in \mathbb{R}^p$; $\hat{S} \subset \{1, \dots, k\}$

- 1 **Initialization :** statsCont:=true; statsIt:=1; $\tilde{\beta}^{r_1} := \mathbf{0}_p$; $\hat{r} := r_M$;
- 2 **while** statsCont==true AND statsIt < M **do**
- 3 statsIt:=statsIt+1;
- 4 compCont:=true;
- 5 betaOld:= $\tilde{\beta}^{r_{\text{statsIt}-1}}$;
- 6 **while** compCont==true **do**
- 7 Compute a feasible dual point $\tilde{\mathbf{v}}^{r_{\text{statsIt}}}$;
- 8 Compute the duality gap $\Delta(\tilde{\beta}^{r_{\text{statsIt}}}, \tilde{\mathbf{v}}^{r_{\text{statsIt}}})$;
- 9 **if** $\Delta(\tilde{\beta}^{r_{\text{statsIt}}}, \tilde{\mathbf{v}}^{r_{\text{statsIt}}}) \leq b$ **then**
- 10 $\tilde{\beta}^{r_{\text{statsIt}}} := \text{betaOld}$;
- 11 compCont:=false;
- 12 **else**
- 13 **for** $j = 1, \dots, k$ **do**
- 14 $\tilde{\beta}_{G^j}^{r_{\text{statsIt}}} := \mathcal{T}_{r_{\text{statsIt}} \sqrt{p_j}/L}(\text{betaOld}_{G^j} - X_{G^j}^\top (X \cdot \text{betaOld} - \mathbf{y})/L)$;
- 15 **end**
- 16 betaOld:= $\tilde{\beta}^{r_{\text{statsIt}}}$;
- 17 **end**
- 18 **end**
- 19 statsCont := $\prod_{i=1}^{\text{statsIt}} \mathbb{1}\left\{ \max_{j \in \{1, \dots, k\}} \|\tilde{\beta}_{G^j}^{r_{\text{statsIt}}} - \tilde{\beta}_{G^j}^{r_i}\|_2 / \sqrt{p_j} (r_{\text{statsIt}} + r_i) - (3/(nc)) \leq 0 \right\}$;
- 20 **end**
- 21 **if** statsCont==false **then**
- 22 $\hat{r} := r_{\text{statsIt}-1}$;
- 23 **end**
- 24 $\hat{S} := \{j \in \{1, \dots, k\} : \|\tilde{\beta}_{G^j}^{\hat{r}}\|_2 / \sqrt{p_j} > 9\hat{r}/(nc)\}$

models with $n = 500$ and $p = 1000$ and with $n = 5000$ and $p = 10000$. Each row of the design matrix $X \in \mathbb{R}^{n \times p}$ is sampled independently from a p -dimensional normal distribution with mean 0 and covariance matrix $(1 - \rho)\mathbf{I} + \rho\mathbb{1}$, where \mathbf{I} is the identity matrix, $\mathbb{1}$ the matrix of ones, and $\rho = 0.3$ the correlation among the features. The design matrix is then normalized such that its columns have Euclidean norm equal to \sqrt{n} . The entries of the noise $\mathbf{u} \in \mathbb{R}^n$ are generated according to a one-dimensional standard normal distribution. The entries of β^* are first set to 0 except for 10 uniformly at random chosen entries that are each set to 1 or -1 with equal probability; the whole vector β^* is then rescaled such that the signal-to-noise ratio $\|X\beta^*\|_2^2/n$ is equal to 5.

For group-FOS, the same setup is used except for the selection of non-zero parameters: the index set is partitioned into groups of equal length, and the non-zero parameters are those in the uniformly at random chosen “active” groups. To obtain a wider range of cases, data size, group lengths, and numbers of activated groups are also modulated.

We summarize the results for feature selection and group-feature selection in Table I and Table II, respectively. For each setting, that is, for each a combination of n , p , group length, and number of activated groups, we recorded the timings of each method. The computational efficiency is measured in average timing (in seconds) over 10 independent runs;

the statistical accuracy is measured in average Hamming distance, which is the sum of the number of false positives and the number of false negatives, and in average estimation error, which is $\|\tilde{\beta}^{\hat{r}} - \beta^*\|_\infty$. If a method timed out on our machines, we put an “NA.” We observe that FOS outperforms lassoCV_{SPAMS}, lassoCV_{glmnet}, SCAD, and MCP and that group-FOS outperforms group-lassoCV_{SPAMS} both in computational efficiency and in statistical accuracy. For large data sets, lassoCV_{SPAMS} and group-lassoCV_{SPAMS} timed out on our machine, which means that the run time for the first run is one hour or more. We also compared FOS with AV approach [7, Algorithm 1] in Table VI (of Appendix B-C).

The two computational benefits of our proposed method are illustrated in Fig. 1. First, we observe that even with warm starts, lassoCV_{SPAMS} requires a large number of iterations to converge. In contrast, FOS allows for early stopping, in particular, for large tuning parameters (recall that the required precision for FOS is proportional to the tuning parameter; instead, the required precision for other methods is unknown). Moreover, Cross-Validation, BIC, AIC, and similar calibration schemes are based on the entire lasso path, while only a part of the path is required for FOS. We should remark that the same result holds for group-FOS.

TABLE I

AVERAGE RUN TIMES (IN SECONDS), HAMMING DISTANCES, AND ESTIMATION ERRORS FOR LASSOCV_{SPAMS}, LASSOCV_{GLMNET}, SCAD, MCP, AND FOS, WITH $M = 100$. FOR THE LARGER DATA SET, LASSOCV_{SPAMS} TIMED OUT ON OUR MACHINE, WHICH MEANS THAT LASSOCV_{SPAMS} TOOK MORE THAN ONE HOUR FOR THE FIRST RUN. THE RESULTS ILLUSTRATE THAT FOS IS BOTH FASTER AND ALMOST MORE ACCURATE THAN OTHER METHODS ACROSS ALL SETTINGS

Method	$n = 500, p = 1000$			$n = 5000, p = 10000$		
	Timing	Hamming distance	Estimation error	Timing	Hamming distance	Estimation error
lassoCV _{SPAMS}	132.72 ± 16.14	71.10 ± 18.17	0.19 ± 0.04	NA	NA	NA
lassoCV _{glmnet}	3.61 ± 1.10	55.10 ± 18.89	0.20 ± 0.04	32.92 ± 7.12	56.80 ± 25.42	0.07 ± 0.01
SCAD	103.50 ± 4.05	70.40 ± 23.51	0.20 ± 0.03	1410.60 ± 87.40	145.40 ± 43.96	0.08 ± 0.00
MCP	100.22 ± 5.84	77.60 ± 19.50	0.19 ± 0.03	1420.60 ± 97.30	139.40 ± 42.15	0.07 ± 0.01
FOS	0.12 ± 0.08	1.00 ± 2.82	0.19 ± 0.04	5.72 ± 2.69	0.00 ± 0.00	0.10 ± 0.02

TABLE II

AVERAGE RUN TIMES (IN SECONDS), HAMMING DISTANCES, AND ESTIMATION ERRORS FOR GROUP-LASSOCV_{SPAMS} AND GROUP-FOS FOR DATA THAT VARY IN GROUP LENGTH (GL) AND NUMBER OF ACTIVATED GROUPS (AG). FOR THE LARGER DATA SET, GROUP-LASSOCV_{SPAMS} TIMED OUT ON OUR MACHINE, WHICH MEANS THAT GROUP-LASSOCV_{SPAMS} TOOK MORE THAN ONE HOUR FOR THE FIRST RUN. THE RESULTS ILLUSTRATE THAT GROUP-FOS IS BOTH FASTER AND ALMOST MORE ACCURATE THAN GROUP-LASSOCV_{SPAMS} ACROSS ALL SETTINGS

Method	$n = 500, p = 1000$			$n = 5000, p = 10000$		
	$GL = 5, AG = 1$			$GL = 5, AG = 40$		
	Timing	Hamming distance	Estimation error	Timing	Hamming distance	Estimation error
group-lassoCV _{SPAMS}	259.25 ± 43.03	133.50 ± 47.15	0.53 ± 0.08	333.87 ± 29.95	671.50 ± 109.31	0.20 ± 0.02
group-FOS	5.14 ± 0.81	0.00 ± 0.00	0.14 ± 0.03	2.88 ± 0.93	195.50 ± 5.50	0.21 ± 0.02
Method	$n = 500, p = 1000$			$n = 5000, p = 10000$		
	$GL = 10, AG = 2$			$GL = 10, AG = 10$		
	Timing	Hamming distance	Estimation error	Timing	Hamming distance	Estimation error
group-lassoCV _{SPAMS}	282.35 ± 41.34	216.00 ± 112.17	0.31 ± 0.06	322.19 ± 33.04	520.00 ± 87.55	0.23 ± 0.02
group-FOS	3.06 ± 0.70	0.00 ± 0.00	0.14 ± 0.01	2.08 ± 0.45	32.00 ± 41.04	0.18 ± 0.01
Method	$n = 5000, p = 10000$			$n = 5000, p = 10000$		
	$GL = 10, AG = 2$			$GL = 10, AG = 10$		
	Timing	Hamming distance	Estimation error	Timing	Hamming distance	Estimation error
group-lassoCV _{SPAMS}	NA	NA	NA	NA	NA	NA
group-FOS	258.19 ± 153.28	2.00 ± 6.32	0.05 ± 0.02	124.97 ± 36.74	2.00 ± 6.32	0.07 ± 0.01

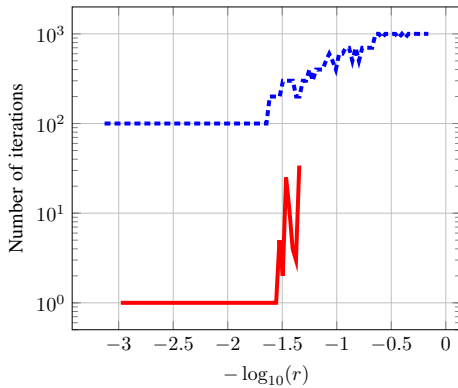


Fig. 1. The red, solid line depicts the number of proximal gradient steps in FOS as a function of the tuning parameter r . The blue, dashed line depicts the corresponding number of proximal gradient steps in lassoCV_{SPAMS}. Shown are the numbers for one data set in the $n = 500$ and $p = 1000$ setting. We observe that lassoCV_{SPAMS} requires a large number of iterations to converge, while FOS allows for early stopping, in particular, for large tuning parameters. Also, lassoCV_{SPAMS} is based on the entire lasso path, while only a part of the path is required for FOS.

b) *Financial data*: Now, we consider a large data set to demonstrate the scalability of FOS. The data [31] comprises $n = 16087$ samples and $p = 150348$ predictors. The goal is to use financial reports of companies to predict the volatility of stock returns. The feature representation of the financial reports is based on the calculation of TF-IDF (term frequency and inverse document frequency) of unigrams. There

is no ground truth available for verifying statistical accuracies, but the data is ideal for verifying the algorithm’s scalability. The computational time of lassoCV_{glmnet} is **124.56s** and of FOS **1.94s**. In contrast, lassoCV_{SPAMS}, SCAD, and MCP timed out on our machine, which again means more than one hour of computation. This shows that our methodology is indeed highly scalable to large data.

c) *Lung cancer data set*: FOS can also be applied to network learning problems by estimating the local neighborhood of each node via high-dimensional regressions. In this specific application, the goal is to understand the interaction network of $p = 1000$ genes in lung cancer patients from $n = 500$ expression profiles [32]. We do neighborhood selection with the “or-rule” [33] based on FOS and lassoCV and compare the estimated graphs with the available gold standard [34]. The results are summarized in Fig. 2. Note that here, the Hamming distance is the sum of the falsely included edges and the falsely omitted edges. We find that our pipeline outmatches the standard one both in speed and accuracy.

d) *Breast cancer data set*: Here, we consider a large data set that contains gene expressions from 60 patients with estrogen-positive breast cancer [35]. The patients were treated for five years and then classified into two categories (labeled by 1 or -1) according to whether the cancer recurred or not. The original data is pre-processed as follows: first, the genes with more than 50 percent missingness are removed

and all other missing values are filled by mean imputation. This reduces number of genes from 22 575 to 12 071. Then, the genes are grouped using cytogenetic position data, namely the C1 set from the GSEA method [36]. The genes that are not recorded in the C1 set are removed, which yields a total of 4989 genes in 270 groups, with an average group size of 18.5 genes. Finally, the data is split via 10-fold Cross-Validation and group-lassoCV_{SPAMS} and group-FOS are applied. The classification is then performed by taking the signum function on the predicted values. We report the classification errors in Fig. 3. We find that group-FOS outperforms group-lassoCV_{SPAMS} in computational efficiency and accuracy.

B. Logistic Regression

Here, we specify our approach to ℓ_1 -regularized logistic regression. In Section III-B1, we provide sufficient conditions for Assumption (1) (see Lemma 7). In Section III-B2, we specify the implementation for feature selection (see Algorithm 3), and in Section III-B3, we demonstrate the empirical efficiency of our approach both on simulated and real data.

1) *Method*: The logistic regression model is

$$\Pr(y_i = 1 | \mathbf{x}_i) = \frac{\exp(\mathbf{x}_i^\top \boldsymbol{\beta}^*)}{1 + \exp(\mathbf{x}_i^\top \boldsymbol{\beta}^*)} \quad i \in \{1, \dots, n\},$$

where $\mathbf{y} = (y_1, \dots, y_n)^\top \in \{0, 1\}^n$ is a binary vector outcome, $\mathbf{x}_1, \dots, \mathbf{x}_n$ are the rows of the design matrix $X \in \mathbb{R}^{n \times p}$, and $\boldsymbol{\beta}^* \in \mathbb{R}^p =: \mathcal{B}$ the regression vector with support $\mathcal{S} = \text{supp}(\boldsymbol{\beta}^*) \subset \{1, \dots, p\}$.

To estimate $\boldsymbol{\beta}^*$, we consider the objective function

$$\ell(\boldsymbol{\beta}, r) := L(\boldsymbol{\beta}) + r \|\boldsymbol{\beta}\|_1, \quad (11)$$

where $\boldsymbol{\beta} \in \mathbb{R}^p$, $r \in [0, \infty) =: \mathcal{R}$, and $L(\boldsymbol{\beta}) := (\sum_{i=1}^n \log(1 + \exp(\mathbf{x}_i^\top \boldsymbol{\beta})) - y_i \mathbf{x}_i^\top \boldsymbol{\beta})/n$. We recall that the ℓ_1 -regularization allows us to control the ℓ_∞ -distance of our estimators. This corresponds in our framework to the measure of accuracy $d(\boldsymbol{\beta}, \boldsymbol{\beta}') := \|\boldsymbol{\beta} - \boldsymbol{\beta}'\|_\infty$. To avoid digression, we focus on ℓ_1 -norm regularization; it is straightforward to extend the results in this section to more general classes of regularizers as in Section III-A. We then propose to use the estimators $\mathcal{F}_\mathcal{R} = \{\tilde{\boldsymbol{\beta}}^r : r \in \mathcal{R}\}$ with

$$\tilde{\boldsymbol{\beta}}^r \in \underset{\boldsymbol{\beta} \in \mathbb{R}^p}{\text{argmin}} \ell(\boldsymbol{\beta}, r). \quad (12)$$

For vectors \mathbf{u}, \mathbf{v} of the same length, we define the function $w(\mathbf{u}, \mathbf{v}) := \exp(\mathbf{u}^\top \mathbf{v}) / (1 + \exp(\mathbf{u}^\top \mathbf{v}))^2$ and we denote by W the diagonal matrix of size $n \times n$ with (i, i) th entry $w(\mathbf{x}_i, \boldsymbol{\beta}^*)$. The residuals are defined as $u_i := y_i - \Pr(y_i = 1 | \mathbf{x}_i)$ for $i \in \{1, \dots, n\}$. A sufficient condition for satisfying the statistical bound in Assumption (1) for estimators in Equation (12) is provided by Li and Lederer [11, Theorem 1] as follows:

Lemma 7 (f in ℓ_1 -regularized logistic regression): Assume

$$e_{\min} := \Omega_{\min}(X_S^\top W X_S / n) > 0 \quad (13)$$

and

$$a := 1 - \|(X_S^\top W X_S)^{-1} X_S^\top W X_{S^c}\|_\infty > 0. \quad (14)$$

Then, $\mathcal{F}_\mathcal{R}$ satisfies

$$\|\boldsymbol{\beta}^* - \tilde{\boldsymbol{\beta}}^r\|_\infty \leq f(r) \quad \forall r \geq r^*$$

for $f(r) := \frac{c_{\log} r}{1.5 \|(X_S^\top W X_S)^{-1}\|_\infty / (\|(X_S^\top W X_S)^{-1}\|_2 e_{\min})}$, and $r^* := 4(2 - a) \|X^\top \mathbf{u}\|_\infty / (na)$.

This result implies that for a suitable tuning parameter r , the estimator $\tilde{\boldsymbol{\beta}}^r$ is uniformly close to the regression vector $\boldsymbol{\beta}^*$. Condition (13) is a modified version of the minimal eigenvalue condition commonly used in the theory for linear regression [24, Equation (11.29)], [11, Assumption 1] and ensures that the relevant covariates are only mildly correlated. Condition (14) is a modified version of irrepresentability condition commonly used in the theories about the lasso [24, Equation (11.27)], [11, Assumption 2], [37] and prevents the relevant covariates from being strongly correlated with the irrelevant covariates. Note that these assumptions are slightly different to (and potentially more stringent than) the assumptions in the linear-regression case; it would be interesting to try relaxing these assumptions—especially in view of our simulations showing that our proposed method performs well even for data with larger correlations (see Appendix B-C)—but this is beyond the scope of the current paper.

A sufficient condition for satisfying the computational bound in Assumption (2) for the estimators in Equation (12) follows again from Lemma 4.

Plugging Lemma 7 and Lemma 4 into Theorem 1 yields the following result.

Corollary 8 (Estimation in ℓ_1 -regularized logistic regression): Suppose that the conditions of Lemma 7 are met and $g = f$. Then, the outputs of Algorithm 1 satisfy

$$\hat{r} \leq r^*,$$

$$\|\tilde{\boldsymbol{\beta}}^{\hat{r}} - \boldsymbol{\beta}^*\|_\infty \leq 6c_{\log} r^*,$$

and

$$\mathbb{E}[\|\tilde{\boldsymbol{\beta}}^{\hat{r}} - \boldsymbol{\beta}^*\|_\infty] \leq \mathbb{E}[6c_{\log} r^*].$$

This equips the proposed algorithm with guarantees for its estimation error in logistic regression.

An estimate of the support is

$$\hat{\mathcal{S}} := \{j \in \{1, \dots, p\} : |\tilde{\boldsymbol{\beta}}_j^{\hat{r}}| > 6c_{\log} \hat{r}\}, \quad (15)$$

where \hat{r} and $\tilde{\boldsymbol{\beta}}^{\hat{r}}$ are the outputs of Algorithm 1. Now, assuming the conditions of Lemma 7 and again a standard beta-min condition

$$\min_{j \in \mathcal{S}} |\boldsymbol{\beta}_j^*| > 12c_{\log} r^*,$$

we obtain a guarantee for $\hat{\mathcal{S}}$.

Corollary 9 (Feature selection in ℓ_1 -regularized logistic regression): Under the stated conditions, it holds that

$$\hat{\mathcal{S}} = \mathcal{S}.$$

Hence, the feature selection scheme in (15) is equipped with a sharp guarantee that takes both the tuning parameter calibration and the computational tolerances of implementations into account.

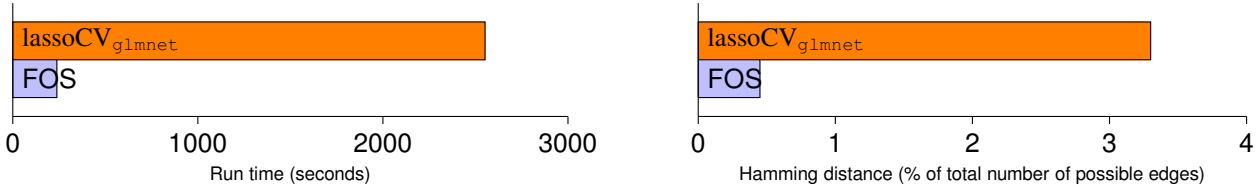


Fig. 2. Run times (in seconds) and Hamming distances (in % of the total number of possible edges) for $\text{lassoCV}_{\text{glmnet}}$ and for FOS on the lung cancer data set. The implementations $\text{lassoCV}_{\text{SPAMS}}$, SCAD, and MCP timed out on our machine. The results illustrate that FOS is both faster and more accurate than $\text{lassoCV}_{\text{glmnet}}$.

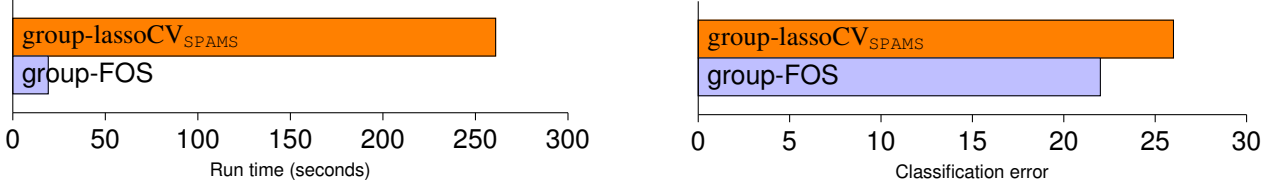


Fig. 3. Run times (in seconds) and classification error for $\text{group-lassoCV}_{\text{SPAMS}}$ and group-FOS on the breast cancer data set illustrate that group-FOS is both faster and more accurate than $\text{group-lassoCV}_{\text{SPAMS}}$.

2) *Algorithm*: Algorithm 3 is a specification of our general scheme for feature selection in ℓ_1 -regularized logistic regression. We call the algorithm log-FOS for convenient reference. The three challenges described earlier are now addressed as follows: (1) The stopping point on the tuning parameter path is determined via AV-tests. (2) To ensure that the computational bound is reached, we follow the same approach as in linear regression case (see Section III-A2). Setting $f(r) := g(r) := c_{\log}r$, which by Lemma 4, gives the stopping criterion as $\Delta(\tilde{\beta}, \tilde{\nu}) \leq b := znr^2(c_{\log} - (1/zn))^2$. (3) We finally use Equation (15) for thresholding, which guarantees correct feature selection (see Corollary 9). As initialization, we choose the all-zeros vector in \mathbb{R}^p , reflecting our assumption that many features are inactive. Since we are limited to finitely many computations in practice, we consider finite sequences $r_1 = r_{\max} > r_2 > \dots > r_M = r_{\min} > 0$. The concrete choice follows the ones used in Li and Lederer [11, Section 3]. We consider $M = 500$ tuning parameters that are equally spaced on $[r_{\min}, r_{\max}]$, where $r_{\min} := 0.0001r_{\max}$ and $r_{\max} := 10 \log(p)/n$ ensure a large spread of outcomes. Finally, $c_{\log} = 6$ and $z = 1$ are considered global constants, see Li and Lederer [11, Section 3] for more details regarding c_{\log} . We show later that changing these constants has minor impact on our results (see Tables X and XI).

3) *Empirical performance*: We now demonstrate the computational efficiency and the empirical accuracy of the proposed method on simulated and real data. We compare log-FOS to the log-lasso with Cross-Validation (log-lassoCV). log-lassoCV is implemented analogously to log-FOS using the SPAMS package and a 10-fold Cross-Validation with warm starts. We call this implementation $\text{log-lassoCV}_{\text{SPAMS}}$.

a) *Synthetic data*: We first use synthetic data to demonstrate the empirical performance of log-FOS. Data are generated from the logistic regression model with $n = 200$ and $p = 200$, $n = 200$ and $p = 500$, and also $n = 1000$ and $p = 5000$. Each row of the design matrix $X \in \mathbb{R}^{n \times p}$ is sampled independently from a p -dimensional normal distribution with mean 0 and covariance matrix $(1 - \rho)\mathbb{I} + \rho\mathbb{1}$, where \mathbb{I}

Algorithm 3: feature selection in ℓ_1 -regularized logistic regression

Inputs : $\mathbf{y} \in \{0, 1\}^n$; $X \in \mathbb{R}^{n \times p}$;
 $r_1 = r_{\max} > r_2 > \dots > r_M > 0$
Outputs: $\tilde{\beta}^{\hat{r}} \in \mathbb{R}^p$; $\hat{\mathcal{S}} \subset \{1, \dots, p\}$

- 1 **Initialization** : $\text{statsCont} := \text{true}$; $\text{statsIt} := 1$;
 $\tilde{\beta}^{r_1} := \mathbf{0}_p$; $\hat{r} := r_M$;
- 2 **while** $\text{statsCont} == \text{true}$ AND $\text{statsIt} < M$ **do**
- 3 $\text{statsIt} := \text{statsIt} + 1$;
- 4 $\text{compCont} := \text{true}$;
- 5 $\text{betaOld} := \tilde{\beta}^{r_{\text{statsIt}-1}}$;
- 6 **while** $\text{compCont} == \text{true}$ **do**
- 7 Compute a feasible dual point $\tilde{\nu}^{r_{\text{statsIt}}}$;
- 8 Compute the duality gap $\Delta(\tilde{\beta}^{r_{\text{statsIt}}}, \tilde{\nu}^{r_{\text{statsIt}}})$;
- 9 **if** $\Delta(\tilde{\beta}^{r_{\text{statsIt}}}, \tilde{\nu}^{r_{\text{statsIt}}}) \leq b$ **then**
- 10 $\tilde{\beta}^{r_{\text{statsIt}}} := \text{betaOld}$;
- 11 $\text{compCont} := \text{false}$;
- 12 **else**
- 13 $\tilde{\beta}^{r_{\text{statsIt}}} :=$ one iteration of Solver applied
to betaOld ;
- 14 $\text{betaOld} := \tilde{\beta}^{r_{\text{statsIt}}}$;
- 15 **end**
- 16 **end**
- 17 $\text{statsCont} := \prod_{i=1}^{\text{statsIt}} \mathbb{1}\{\|\tilde{\beta}^{r_{\text{statsIt}}}\|_{\infty} - \tilde{\beta}^{r_i}\|_{\infty} / (r_{\text{statsIt}} + r_i) - 2c_{\log} \leq 0\}$;
- 18 **end**
- 19 **if** $\text{statsCont} == \text{false}$ **then**
- 20 $\hat{r} := r_{\text{statsIt}-1}$;
- 21 **end**
- 22 $\hat{\mathcal{S}} := \{j \in \{1, \dots, p\} : |\tilde{\beta}_j^{\hat{r}}| > 6c_{\log}\hat{r}\}$

is the identity matrix, $\mathbb{1}$ the matrix of ones, and $\rho \in \{0.25, 0.5\}$

the population correlation among the features. The design matrix is then normalized such that its columns have Euclidean norm equal to \sqrt{n} . The entries of β^* are first set to 0 except for $s = 8$ uniformly at random chosen entries that are set to 1 or -1 with equal probability. The computational efficiency is measured in average timing (in seconds) over 10 independent runs; the statistical accuracy is measured in average Hamming distance and in average estimation error, which is $\|\tilde{\beta}^{\hat{r}} - \beta^*\|_\infty$. Table III reports the results for data generated with different size and correlation. We find that log-FOS outperforms log-lassoCV_{SPAMS} in computational efficiency and accuracy even for data with high correlation. The results for the other correlation and sparsity levels are deferred to the Appendix B-C. We also compared log-FOS with Li and Lederer [11] in Table VII (of Appendix B-C).

b) Melanoma patients: We compare the performance of log-FOS against log-lassoCV_{SPAMS} classifying melanoma patients [38], including $n = 205$ mass spectrometry scans of serum samples collected from 101 patients with early-stage melanoma and 104 patients with advanced stage melanoma. Each scan measures the intensities for 18 856 mass over charge (m/Z) values. Finding m/Z values associated with the stage of the disease is of our interest for classifying data. We fit a logistic regression model with the same data pre-processing step as in Lederer and Müller [39]: We start with a peak filtering algorithm to extract $p = 500$ most relevant m/Z values. We also fill $\mathbf{y} \in \{-1, 1\}^{205}$ with $y_i = -1$ for $i = 1, \dots, 101$ (early-stage) and $y_i = 1$ for $i = 102, \dots, 205$ (advanced stage). Finally, we use 10-fold Cross-Validation splitting data and log-lassoCV_{SPAMS} and log-FOS are applied. Fig. 4 reports the mean 10-fold CV classification errors by log-FOS and log-lassoCV_{SPAMS}, as well as their run times. We find that log-FOS outperforms log-lassoCV_{SPAMS} in computational efficiency and accuracy.

IV. DISCUSSION

In view of the theoretical and empirical evidence provided above, the presented approach provides competitive methods for feature selection and group-feature selection with large and high-dimensional data. In particular, there are no comparable theoretical guarantees that provide a connection between statistical and computational accuracy, and in our simulations and real data applications, the algorithm rivals or outmatches its competitors in terms of speed and accuracy.

Our theories do not discuss the optimal choice of the set of tuning parameters over which to optimize; this might be a direction for future research.

APPENDIX A PROOFS

We provide proofs of our main results and derive one property of vectors that are close to a solution $\tilde{\beta}^r$ of (9) and (12): in Lemma 12, we show that their error belongs to a cone.

Proof [Theorem 1] We prove the three claims in order.

Claim 1: We first prove that $\hat{r} \leq r^*$. We show this by

contradiction and assume that $\hat{r} > r^*$. By definition of \hat{r} , this means that there are tuning parameters $r', r'' \geq r^*$ such that

$$d(\tilde{\beta}^{r'}, \tilde{\beta}^{r''}) > f(r') + g(r') + f(r'') + g(r'').$$

On the other hand, by the assumed symmetry and triangle inequality of d , it holds that

$$d(\tilde{\beta}^{r'}, \tilde{\beta}^{r''}) \leq d(\tilde{\beta}^{r'}, \beta^*) + d(\tilde{\beta}^{r''}, \beta^*).$$

Using the symmetry and triangle inequality of d again and combining with Assumptions (1) and (2) (statistical and computational bounds) yields for the first term

$$d(\tilde{\beta}^{r'}, \beta^*) \leq d(\tilde{\beta}^{r'}, \beta^*) + d(\tilde{\beta}^{r'}, \tilde{\beta}^{r'}) \leq f(r') + g(r'),$$

and similarly for the second term

$$d(\tilde{\beta}^{r''}, \beta^*) \leq f(r'') + g(r'').$$

It follows that

$$d(\tilde{\beta}^{r'}, \tilde{\beta}^{r''}) \leq f(r') + g(r') + f(r'') + g(r''),$$

which contradicts the initial display, and thus concludes the proof of the first inequality.

Claim 2: We now prove that

$$d(\tilde{\beta}^{\hat{r}}, \beta^*) \leq 3f(r^*) + 3g(r^*).$$

For this, we first use the symmetry and triangle inequality of d to find

$$d(\tilde{\beta}^{\hat{r}}, \beta^*) \leq d(\tilde{\beta}^{r^*}, \beta^*) + d(\tilde{\beta}^{r^*}, \tilde{\beta}^{\hat{r}}).$$

The first term can be bounded similarly as in Claim 1. We find

$$d(\tilde{\beta}^{r^*}, \beta^*) \leq f(r^*) + g(r^*).$$

The second term can be bounded by virtue of the definition of the test and $\hat{r} \leq r^*$ according to the Claim 1. We find

$$d(\tilde{\beta}^{r^*}, \tilde{\beta}^{\hat{r}}) \leq f(r^*) + g(r^*) + f(\hat{r}) + g(\hat{r}).$$

We can now combine the terms and use that $\hat{r} \leq r^*$ and that f, g are increasing to find

$$d(\tilde{\beta}^{\hat{r}}, \beta^*) \leq 3f(r^*) + 3g(r^*),$$

as desired.

Claim 3: We finally prove that

$$\mathbb{E}[d(\tilde{\beta}^{\hat{r}}, \beta^*)] \leq 3\mathbb{E}f(r^*) + 3\mathbb{E}g(r^*).$$

This follows directly from Claim 2 by taking expectations. ■

Lemma 10 (Relaxed guarantee for \hat{r} and $\tilde{\beta}^{\hat{r}}$): Under Assumption 1, any estimator $\tilde{\beta}^r$, $r \geq \hat{r}$ with \hat{r} from Algorithm 1, satisfies

$$d(\tilde{\beta}^r, \beta^*) \leq 3f(\max\{r^*, r\}) + 3g(\max\{r^*, r\}).$$

Proof [Lemma 10]

By the symmetry and triangle inequality of d ,

$$d(\tilde{\beta}^r, \beta^*) \leq d(\tilde{\beta}^{r^*}, \beta^*) + d(\tilde{\beta}^{r^*}, \tilde{\beta}^r).$$

TABLE III

AVERAGE RUN TIMES (IN SECONDS), HAMMING DISTANCES, AND ESTIMATION ERRORS FOR LOG-LASSO CV_{SPAMS} AND LOG-FOS, WITH $M = 500$. FOR LARGE DATA SET, LOG-LASSO CV_{SPAMS} TIMED OUT ON OUR MACHINE, WHICH MEANS THAT LOG-LASSO CV_{SPAMS} TOOK MORE THAN ONE HOUR FOR THE FIRST RUN. THE RESULTS ILLUSTRATE THAT LOG-FOS IS BOTH FASTER AND MORE ACCURATE THAN LOG-LASSO CV_{SPAMS} ACROSS ALL SETTINGS

$n = 200, p = 200, s = 8$						
Method	$\rho = 0.25$			$\rho = 0.5$		
	Timing	Hamming distance	Estimation error	Timing	Hamming distance	Estimation error
log-lasso CV_{SPAMS}	13.96 ± 0.59	7.80 ± 3.04	2.89 ± 0.57	15.77 ± 0.33	10.80 ± 2.29	2.96 ± 0.57
log-FOS	0.36 ± 0.06	3.10 ± 1.79	2.04 ± 0.59	0.58 ± 0.03	5.60 ± 2.11	2.35 ± 0.69
$n = 200, p = 500, s = 8$						
Method	$\rho = 0.25$			$\rho = 0.5$		
	Timing	Hamming distance	Estimation error	Timing	Hamming distance	Estimation error
log-lasso CV_{SPAMS}	26.12 ± 0.58	11.10 ± 4.38	3.17 ± 0.20	26.48 ± 0.66	13.90 ± 3.87	3.32 ± 0.21
log-FOS	1.22 ± 0.07	4.40 ± 1.95	2.36 ± 0.16	1.09 ± 0.04	8.60 ± 3.83	2.56 ± 0.36
$n = 1000, p = 5000, s = 8$						
Method	$\rho = 0.25$			$\rho = 0.5$		
	Timing	Hamming distance	Estimation error	Timing	Hamming distance	Estimation error
log-lasso CV_{SPAMS}	NA	NA	NA	NA	NA	NA
log-FOS	33.64 ± 4.69	4.70 ± 1.33	2.48 ± 0.58	25.95 ± 4.23	3.80 ± 1.68	2.54 ± 0.57

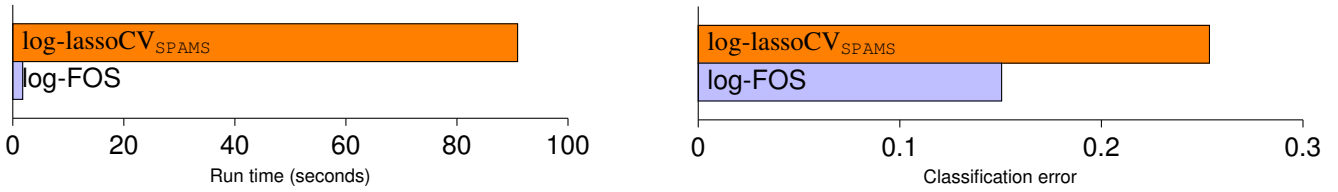


Fig. 4. Run times (in seconds) and classification error for log-lasso CV_{SPAMS} and log-FOS on the melanoma patients illustrate that log-FOS is both faster and more accurate than log-lasso CV_{SPAMS} .

The first term can be bounded as in the earlier proof:

$$d(\tilde{\beta}^{r^*}, \beta^*) \leq f(r^*) + g(r^*).$$

For the second term, we use that $\hat{r} \leq r, r^*$ by assumption/earlier proof and the tests in Algorithm 1 to deduce that

$$d(\tilde{\beta}^{r^*}, \tilde{\beta}^r) \leq f(r^*) + g(r^*) + f(r) + g(r).$$

Collecting the pieces and using and that f, g are increasing yields

$$d(\tilde{\beta}^r, \beta^*) \leq 3f(\max\{r^*, r\}) + 3g(\max\{r^*, r\}),$$

as desired. \blacksquare

Proof [Lemma 2] We will first prove that $\hat{\mathcal{S}}^{\mathbb{C}} \subset \mathcal{S}^{\mathbb{C}}$. For this, consider $j \in \hat{\mathcal{S}}^{\mathbb{C}}$ and note that by the triangle inequality

$$\begin{aligned} \|\beta_{G^j}^*\|_q &= \|\beta_{G^j}^* - \tilde{\beta}_{G^j}^{\hat{r}} + \tilde{\beta}_{G^j}^{\hat{r}}\|_q \\ &\leq \|\beta_{G^j}^* - \tilde{\beta}_{G^j}^{\hat{r}}\|_q + \|\tilde{\beta}_{G^j}^{\hat{r}}\|_q. \end{aligned}$$

The first term can be bounded by using Theorem 1, Result (4):

$$\|\beta_{G^j}^* - \tilde{\beta}_{G^j}^{\hat{r}}\|_q \leq \|\beta^* - \tilde{\beta}^{\hat{r}}\|_{q, \infty} \leq 3f(r^*) + 3g(r^*).$$

The second term can be bounded by using $j \in \hat{\mathcal{S}}^{\mathbb{C}}$ and the definition of $\hat{\mathcal{S}}$:

$$\|\tilde{\beta}_{G^j}^{\hat{r}}\|_q \leq 3f(\hat{r}) + 3g(\hat{r}).$$

Collecting the pieces and using that $\hat{r} \leq r^*$ (Theorem 1, Result (3)) gives

$$\begin{aligned} \|\beta_{G^j}^*\|_q &\leq 3f(r^*) + 3g(r^*) + 3f(r^*) + 3g(r^*) \\ &= 6f(r^*) + 6g(r^*), \end{aligned}$$

which means by virtue of the beta-min condition that $j \in \mathcal{S}^{\mathbb{C}}$. This concludes the proof of the first part.

Next, we prove that $\mathcal{S}^{\mathbb{C}} \subset \hat{\mathcal{S}}^{\mathbb{C}}$. Using $j \in \mathcal{S}^{\mathbb{C}}$, that is $\beta_{G^j}^* = \mathbf{0}_{p_j}$, we obtain

$$\|\tilde{\beta}_{G^j}^{\hat{r}}\|_q = \|\tilde{\beta}_{G^j}^{\hat{r}} - \beta_{G^j}^*\|_q \leq 3f(r^*) + 3g(r^*),$$

where the inequality is obtained similarly to the first part of the proof. \blacksquare

Lemma 11 (Subdifferential of regularizer): For all $\kappa' \in \partial\|\beta'\|^\dagger$, where $\partial\|\beta'\|^\dagger$ is the subdifferential of the regularizer at $\beta' \in \mathbb{R}^p$, we have $\|\kappa'\| \leq 1$ (recall that $\|\cdot\|$ is the dual norm of $\|\cdot\|^\dagger$).

Proof [Lemma 11] We prove that $\|\kappa'\| \leq 1$ for all $\kappa' \in \partial\|\beta'\|^\dagger$. Since $\kappa' \in \partial\|\beta'\|^\dagger$, by definition we have for all $\beta \in \mathbb{R}^p$

$$\|\beta\|^\dagger \geq \|\beta'\|^\dagger + \langle \kappa', \beta - \beta' \rangle$$

and by some rearranging we have

$$\langle \kappa', \beta' \rangle - \|\beta'\|^\dagger \geq \langle \kappa', \beta \rangle - \|\beta\|^\dagger.$$

Because above inequality holds for all $\beta \in \mathbb{R}^p$, we also obtain

$$\langle \kappa', \beta' \rangle - \|\beta'\|^\dagger \geq \sup_{\beta \in \mathbb{R}^p} \{ \langle \kappa', \beta \rangle - \|\beta\|^\dagger \}.$$

The right hand side of the inequality above represents the Fenchel conjugate of $\|\cdot\|^\dagger$ at $\boldsymbol{\kappa}'$. We use Bach et al. [40, Proposition 1.4] to obtain

$$\begin{aligned} \langle \boldsymbol{\kappa}', \boldsymbol{\beta}' \rangle - \|\boldsymbol{\beta}'\|^\dagger &\geq \sup_{\boldsymbol{\beta} \in \mathbb{R}^p} \{ \langle \boldsymbol{\kappa}', \boldsymbol{\beta} \rangle - \|\boldsymbol{\beta}\|^\dagger \} \\ &= \begin{cases} 0 & \|\boldsymbol{\kappa}'\| \leq 1; \\ +\infty & \text{otherwise.} \end{cases} \end{aligned}$$

The left-hand side of the display is finite for each given $\boldsymbol{\beta}', \boldsymbol{\kappa}'$; hence, it must hold that $\|\boldsymbol{\kappa}'\| \leq 1$.

Proof [Lemma 3] We prove the result in two steps.

Step 1: We first prove that $\boldsymbol{\delta} := \boldsymbol{\beta}^* - \bar{\boldsymbol{\beta}}^r$ satisfies

$$\|\boldsymbol{\delta}_{\mathcal{S}^c}\|^\dagger \leq 3\|\boldsymbol{\delta}_{\mathcal{S}}\|^\dagger.$$

By definition of $\bar{\boldsymbol{\beta}}^r$, we find the basic inequality

$$\frac{1}{2}\|\mathbf{y} - X\boldsymbol{\beta}^*\|_2^2 + r\|\boldsymbol{\beta}^*\|^\dagger \geq \frac{1}{2}\|\mathbf{y} - X\bar{\boldsymbol{\beta}}^r\|_2^2 + r\|\bar{\boldsymbol{\beta}}^r\|^\dagger.$$

We can now rewrite $\|\mathbf{y} - X\bar{\boldsymbol{\beta}}^r\|_2^2/2$ as follows:

$$\begin{aligned} &\frac{1}{2}\|\mathbf{y} - X\bar{\boldsymbol{\beta}}^r\|_2^2 \\ &= \frac{1}{2}\|\mathbf{y} - X\boldsymbol{\beta}^* + X\boldsymbol{\beta}^* - X\bar{\boldsymbol{\beta}}^r\|_2^2 \\ &= \frac{1}{2}\|\mathbf{y} - X\boldsymbol{\beta}^*\|_2^2 + \langle \mathbf{y} - X\boldsymbol{\beta}^*, X\boldsymbol{\beta}^* - X\bar{\boldsymbol{\beta}}^r \rangle \\ &\quad + \frac{1}{2}\|X\boldsymbol{\beta}^* - X\bar{\boldsymbol{\beta}}^r\|_2^2 \\ &= \frac{1}{2}\|\mathbf{y} - X\boldsymbol{\beta}^*\|_2^2 + \langle X^\top(\mathbf{y} - X\boldsymbol{\beta}^*), \boldsymbol{\beta}^* - \bar{\boldsymbol{\beta}}^r \rangle \\ &\quad + \frac{1}{2}\|X\boldsymbol{\beta}^* - X\bar{\boldsymbol{\beta}}^r\|_2^2. \end{aligned}$$

Combining the two displays yields

$$r\|\boldsymbol{\beta}^*\|^\dagger \geq \langle X^\top(\mathbf{y} - X\boldsymbol{\beta}^*), \boldsymbol{\beta}^* - \bar{\boldsymbol{\beta}}^r \rangle + \frac{1}{2}\|X\boldsymbol{\beta}^* - X\bar{\boldsymbol{\beta}}^r\|_2^2 + r\|\bar{\boldsymbol{\beta}}^r\|^\dagger.$$

We now use that $\|X\boldsymbol{\beta}^* - X\bar{\boldsymbol{\beta}}^r\|_2^2/2 \geq 0$ and invoke the model $\mathbf{y} = X\boldsymbol{\beta}^* + \mathbf{u}$ to find

$$r\|\boldsymbol{\beta}^*\|^\dagger \geq \langle X^\top\mathbf{u}, \boldsymbol{\beta}^* - \bar{\boldsymbol{\beta}}^r \rangle + r\|\bar{\boldsymbol{\beta}}^r\|^\dagger.$$

This can be rearranged to

$$r\|\bar{\boldsymbol{\beta}}^r\|^\dagger \leq \langle X^\top\mathbf{u}, \bar{\boldsymbol{\beta}}^r - \boldsymbol{\beta}^* \rangle + r\|\boldsymbol{\beta}^*\|^\dagger.$$

Invoking Hölder's inequality and the assumption that $r \geq 2\|X^\top\mathbf{u}\|$ provides us with

$$\begin{aligned} \langle X^\top\mathbf{u}, \bar{\boldsymbol{\beta}}^r - \boldsymbol{\beta}^* \rangle &\leq \|X^\top\mathbf{u}\|\|\bar{\boldsymbol{\beta}}^r - \boldsymbol{\beta}^*\|^\dagger \\ &\leq \frac{r}{2}\|\bar{\boldsymbol{\beta}}^r - \boldsymbol{\beta}^*\|^\dagger. \end{aligned}$$

Together with the above inequality, we thus find

$$r\|\bar{\boldsymbol{\beta}}^r\|^\dagger \leq \frac{r}{2}\|\bar{\boldsymbol{\beta}}^r - \boldsymbol{\beta}^*\|^\dagger + r\|\boldsymbol{\beta}^*\|^\dagger.$$

We then divide both sides by $r \in (0, \infty)$ and find

$$\|\bar{\boldsymbol{\beta}}^r\|^\dagger \leq \frac{1}{2}\|\bar{\boldsymbol{\beta}}^r - \boldsymbol{\beta}^*\|^\dagger + \|\boldsymbol{\beta}^*\|^\dagger.$$

According to the assumed decomposability of $\|\cdot\|^\dagger$ with respect to \mathcal{S} , we can now decompose each of these vectors into their parts on \mathcal{S} and \mathcal{S}^c :

$$\begin{aligned} \|\bar{\boldsymbol{\beta}}_{\mathcal{S}}^r\|^\dagger + \|\bar{\boldsymbol{\beta}}_{\mathcal{S}^c}^r\|^\dagger &\leq \frac{1}{2}\|\bar{\boldsymbol{\beta}}_{\mathcal{S}}^r - \boldsymbol{\beta}_{\mathcal{S}}^*\|^\dagger + \frac{1}{2}\|\bar{\boldsymbol{\beta}}_{\mathcal{S}^c}^r - \boldsymbol{\beta}_{\mathcal{S}^c}^*\|^\dagger \\ &\quad + \|\boldsymbol{\beta}_{\mathcal{S}}^*\|^\dagger + \|\boldsymbol{\beta}_{\mathcal{S}^c}^*\|^\dagger \\ &= \frac{1}{2}\|\bar{\boldsymbol{\beta}}_{\mathcal{S}}^r - \boldsymbol{\beta}_{\mathcal{S}}^*\|^\dagger + \frac{1}{2}\|\bar{\boldsymbol{\beta}}_{\mathcal{S}^c}^r\|^\dagger + \|\boldsymbol{\beta}_{\mathcal{S}}^*\|^\dagger. \end{aligned}$$

We can rearrange the terms and find

$$\frac{1}{2}\|\bar{\boldsymbol{\beta}}_{\mathcal{S}^c}^r\|^\dagger \leq \frac{1}{2}\|\bar{\boldsymbol{\beta}}_{\mathcal{S}}^r - \boldsymbol{\beta}_{\mathcal{S}}^*\|^\dagger + \|\boldsymbol{\beta}_{\mathcal{S}}^*\|^\dagger - \|\bar{\boldsymbol{\beta}}_{\mathcal{S}}^r\|^\dagger.$$

Using the reverse triangle inequality, this becomes

$$\frac{1}{2}\|\bar{\boldsymbol{\beta}}_{\mathcal{S}^c}^r\|^\dagger \leq \frac{3}{2}\|\bar{\boldsymbol{\beta}}_{\mathcal{S}}^r - \boldsymbol{\beta}_{\mathcal{S}}^*\|^\dagger.$$

Finally, setting $\boldsymbol{\delta} := \boldsymbol{\beta}^* - \bar{\boldsymbol{\beta}}^r$ and multiplying both sides by 2 gives the desired inequality

$$\|\boldsymbol{\delta}_{\mathcal{S}^c}\|^\dagger \leq 3\|\boldsymbol{\delta}_{\mathcal{S}}\|^\dagger.$$

Step 2: We now prove that $\mathcal{F}_{\mathcal{R}}$ satisfies

$$\|\boldsymbol{\beta}^* - \bar{\boldsymbol{\beta}}^r\| \leq \frac{3r}{2nc} \quad \text{for all } r \geq 2\|X^\top\mathbf{u}\|.$$

For this, we first observe that the KKT conditions for the objective function at $\bar{\boldsymbol{\beta}}^r$ are

$$-X^\top(\mathbf{y} - X\bar{\boldsymbol{\beta}}^r) + r\bar{\boldsymbol{\kappa}} = \mathbf{0}_p,$$

where $\bar{\boldsymbol{\kappa}} \in \partial\|\bar{\boldsymbol{\beta}}^r\|^\dagger$ (where $\partial\|\bar{\boldsymbol{\beta}}^r\|^\dagger$ is the subdifferential of regularizer at $\bar{\boldsymbol{\beta}}^r$). Using the model, we have

$$-X^\top(X\boldsymbol{\beta}^* + \mathbf{u} - X\bar{\boldsymbol{\beta}}^r) + r\bar{\boldsymbol{\kappa}} = \mathbf{0}_p,$$

and rearranging yields

$$X^\top X(\boldsymbol{\beta}^* - \bar{\boldsymbol{\beta}}^r) = r\bar{\boldsymbol{\kappa}} - X^\top\mathbf{u}.$$

Applying the norm on both sides and using the linearity and triangle inequality for norms gives

$$\begin{aligned} \|X^\top X(\boldsymbol{\beta}^* - \bar{\boldsymbol{\beta}}^r)\| &= \|r\bar{\boldsymbol{\kappa}} - X^\top\mathbf{u}\| \\ &\leq r\|\bar{\boldsymbol{\kappa}}\| + \|X^\top\mathbf{u}\|. \end{aligned}$$

Using now that $\|\bar{\boldsymbol{\kappa}}\| \leq 1$ ($\bar{\boldsymbol{\kappa}} \in \partial\|\bar{\boldsymbol{\beta}}^r\|^\dagger$ and we use our Lemma 11) and $r \geq 2\|X^\top\mathbf{u}\|$ (by assumption) gives

$$\|X^\top X(\boldsymbol{\beta}^* - \bar{\boldsymbol{\beta}}^r)\| \leq r + \frac{r}{2} = \frac{3r}{2}.$$

Now, we recall that $\boldsymbol{\delta} := \boldsymbol{\beta}^* - \bar{\boldsymbol{\beta}}^r$ satisfies $\|\boldsymbol{\delta}_{\mathcal{S}^c}\|^\dagger \leq 3\|\boldsymbol{\delta}_{\mathcal{S}}\|^\dagger$ according to Step 1. Thus, the assumption given in the lemma entails $\|\boldsymbol{\beta}^* - \bar{\boldsymbol{\beta}}^r\| \leq \|X^\top X(\boldsymbol{\beta}^* - \bar{\boldsymbol{\beta}}^r)\|/(nc)$, so that

$$\|\boldsymbol{\beta}^* - \bar{\boldsymbol{\beta}}^r\| \leq \frac{3r}{2nc},$$

as desired. \blacksquare

Lemma 12 (Cone constraint in regularized regression): Let $b \in [0, \infty)$ be a constant and $\tilde{\boldsymbol{\beta}} \in \mathbb{R}^p$ any vector that satisfies $\ell(\tilde{\boldsymbol{\beta}}, 2r) \leq \ell(\tilde{\boldsymbol{\beta}}^r, 2r) + b$. Then $\boldsymbol{\delta} := \tilde{\boldsymbol{\beta}} - \tilde{\boldsymbol{\beta}}^r$ belongs to the cone

$$\mathcal{C}(\mathcal{S}) := \left\{ \boldsymbol{\nu} \in \mathbb{R}^p : \|\boldsymbol{\nu}_{\mathcal{S}^c}\|^\dagger \leq 3\|\boldsymbol{\nu}_{\mathcal{S}}\|^\dagger + 4\|\bar{\boldsymbol{\beta}}_{\mathcal{S}^c}^r\|^\dagger + \frac{b}{r} \right\}.$$

Proof [Lemma 12] Since $\ell(\tilde{\beta}, 2r) \leq \ell(\bar{\beta}^r, 2r) + b$, we find the basic inequality

$$L(\bar{\beta}^r + \delta) + 2r\|\bar{\beta}^r + \delta\|^\dagger \leq L(\bar{\beta}^r) + 2r\|\bar{\beta}^r\|^\dagger + b.$$

This inequality is equivalent to

$$L(\bar{\beta}^r + \delta) - L(\bar{\beta}^r) + 2r\|\bar{\beta}^r + \delta\|^\dagger - 2r\|\bar{\beta}^r\|^\dagger \leq b.$$

Next, we find a lower bound for the left-hand side of the above display in two steps:

Step 1: First, we show that

$$L(\bar{\beta}^r + \delta) - L(\bar{\beta}^r) \geq -r(\|\delta_S\|^\dagger + \|\delta_{S^c}\|^\dagger).$$

By convexity of the loss function L , we have

$$L(\bar{\beta}^r + \delta) - L(\bar{\beta}^r) \geq \langle \nabla L(\bar{\beta}^r), \delta \rangle \geq -|\langle \nabla L(\bar{\beta}^r), \delta \rangle|.$$

The KKT condition for $\bar{\beta}^r$ provides us with $\nabla L(\bar{\beta}^r) = -r\bar{\kappa}$, for some vector $\bar{\kappa} \in \partial\|\bar{\beta}^r\|^\dagger$. Invoking Hölder's inequality, applying the decomposability of $\|\cdot\|^\dagger$ with respect to \mathcal{S} , and using that $\|\bar{\kappa}\| \leq 1$ (by Lemma 11) yields

$$\begin{aligned} L(\bar{\beta}^r + \delta) - L(\bar{\beta}^r) &\geq -r\|\bar{\kappa}\|(\|\delta_S\|^\dagger + \|\delta_{S^c}\|^\dagger) \\ &\geq -r(\|\delta_S\|^\dagger + \|\delta_{S^c}\|^\dagger). \end{aligned}$$

Step 2: Now we prove that

$$\|\bar{\beta}^r + \delta\|^\dagger - \|\bar{\beta}^r\|^\dagger \geq \|\delta_{S^c}\|^\dagger - 2\|\bar{\beta}_{S^c}^r\|^\dagger - \|\delta_S\|^\dagger.$$

Using that $\|\bar{\beta}^r + \delta\|^\dagger = \|\bar{\beta}_S^r + \bar{\beta}_{S^c}^r + \delta_S + \delta_{S^c}\|^\dagger$ and applying the triangle inequality gives

$$\|\bar{\beta}^r + \delta\|^\dagger \geq \|\bar{\beta}_S^r + \delta_{S^c}\|^\dagger - \|\bar{\beta}_{S^c}^r + \delta_S\|^\dagger.$$

Subtracting $\|\bar{\beta}^r\|^\dagger$ from both sides of the above inequality and using decomposability condition, we obtain

$$\begin{aligned} \|\bar{\beta}^r + \delta\|^\dagger - \|\bar{\beta}^r\|^\dagger &\geq \|\bar{\beta}_S^r + \delta_{S^c}\|^\dagger - \|\bar{\beta}_{S^c}^r + \delta_S\|^\dagger - \|\bar{\beta}^r\|^\dagger \\ &= \|(\bar{\beta}_S^r + \delta_{S^c})_S\|^\dagger + \|(\bar{\beta}_{S^c}^r + \delta_S)_{S^c}\|^\dagger \\ &\quad - \|(\bar{\beta}_{S^c}^r + \delta_S)_S\|^\dagger - \|(\bar{\beta}_S^r + \delta_{S^c})_{S^c}\|^\dagger - \|\bar{\beta}^r\|^\dagger \\ &= \|\bar{\beta}_S^r\|^\dagger + \|\delta_{S^c}\|^\dagger - \|\bar{\beta}_{S^c}^r\|^\dagger - \|\delta_S\|^\dagger \\ &\quad - \|\bar{\beta}_S^r\|^\dagger - \|\bar{\beta}_{S^c}^r\|^\dagger \\ &= \|\delta_{S^c}\|^\dagger - 2\|\bar{\beta}_{S^c}^r\|^\dagger - \|\delta_S\|^\dagger. \end{aligned}$$

Combining the results of Step 1 and Step 2 gives

$$\begin{aligned} L(\bar{\beta}^r + \delta) - L(\bar{\beta}^r) + 2r\|\bar{\beta}^r + \delta\|^\dagger - 2r\|\bar{\beta}^r\|^\dagger \\ \geq -r(\|\delta_S\|^\dagger + \|\delta_{S^c}\|^\dagger) + 2r\|\delta_{S^c}\|^\dagger \\ \quad - 4r\|\bar{\beta}_{S^c}^r\|^\dagger - 2r\|\delta_S\|^\dagger \\ = r\|\delta_{S^c}\|^\dagger - 3r\|\delta_S\|^\dagger - 4r\|\bar{\beta}_{S^c}^r\|^\dagger. \end{aligned}$$

Finally, plugging this into the basic inequality and rearranging, we find

$$\|\delta_{S^c}\|^\dagger \leq 3\|\delta_S\|^\dagger + 4\|\bar{\beta}_{S^c}^r\|^\dagger + \frac{b}{r},$$

as desired. \blacksquare

Proof [Lemma 4] Since $\ell(\tilde{\beta}, 2r) \leq \ell(\bar{\beta}^r, 2r) + b$, we find the basic inequality

$$L(\tilde{\beta}) + 2r\|\tilde{\beta}\|^\dagger \leq L(\bar{\beta}^r) + 2r\|\bar{\beta}^r\|^\dagger + b.$$

We now recall that the KKT conditions read

$$\nabla L(\bar{\beta}^r) + r\bar{\kappa} = \mathbf{0}_p,$$

for some vector $\bar{\kappa} \in \partial\|\bar{\beta}^r\|^\dagger$. Adding a null term to the right-hand side of the previous display gives

$$\begin{aligned} L(\tilde{\beta}) + 2r\|\tilde{\beta}\|^\dagger &\leq L(\bar{\beta}^r) + 2r\|\bar{\beta}^r\|^\dagger + b \\ &\quad + \langle \nabla L(\bar{\beta}^r) + r\bar{\kappa}, \tilde{\beta} - \bar{\beta}^r \rangle. \end{aligned}$$

Rearranging yields

$$\begin{aligned} L(\tilde{\beta}) - L(\bar{\beta}^r) - \langle \nabla L(\bar{\beta}^r), \tilde{\beta} - \bar{\beta}^r \rangle \\ \leq \langle r\bar{\kappa}, \tilde{\beta} - \bar{\beta}^r \rangle - 2r\|\tilde{\beta}\|^\dagger + 2r\|\bar{\beta}^r\|^\dagger + b. \end{aligned}$$

Using that $\|\bar{\kappa}\| \leq 1$ (Lemma 11) and $\bar{\kappa}^\top \bar{\beta}^r = \|\bar{\beta}^r\|^\dagger$, we get

$$\begin{aligned} L(\tilde{\beta}) - L(\bar{\beta}^r) - \langle \nabla L(\bar{\beta}^r), \tilde{\beta} - \bar{\beta}^r \rangle \\ \leq r(\bar{\kappa}^\top \tilde{\beta} - \|\tilde{\beta}\|^\dagger) - r\|\tilde{\beta}\|^\dagger + r\|\bar{\beta}^r\|^\dagger + b, \end{aligned}$$

and by Hölder's inequality, $\bar{\kappa}^\top \tilde{\beta} \leq \|\bar{\kappa}\|\|\tilde{\beta}\|^\dagger \leq \|\tilde{\beta}\|^\dagger$. Therefore,

$$L(\tilde{\beta}) - L(\bar{\beta}^r) - \langle \nabla L(\bar{\beta}^r), \tilde{\beta} - \bar{\beta}^r \rangle \leq r\|\bar{\beta}^r\|^\dagger - r\|\tilde{\beta}\|^\dagger + b,$$

so that with the reverse triangle inequality

$$L(\tilde{\beta}) - L(\bar{\beta}^r) - \langle \nabla L(\bar{\beta}^r), \tilde{\beta} - \bar{\beta}^r \rangle \leq r\|\tilde{\beta} - \bar{\beta}^r\|^\dagger + b.$$

We finally get, setting $\delta := \tilde{\beta} - \bar{\beta}^r$,

$$L(\bar{\beta}^r + \delta) - L(\bar{\beta}^r) - \langle \nabla L(\bar{\beta}^r), \delta \rangle \leq r\|\delta\|^\dagger + b.$$

Moreover, Lemma 12 guarantees that $\delta \in \mathcal{C}(\mathcal{S})$ and thus allows us to apply the condition in the upper display of the lemma. So we also find

$$L(\bar{\beta}^r + \delta) - L(\bar{\beta}^r) - \langle \nabla L(\bar{\beta}^r), \delta \rangle \geq zn\|\delta\|^{2z}.$$

Combining these two inequalities gives us

$$zn\|\delta\|^{2z} \leq r\|\delta\|^\dagger + b.$$

Dividing both sides of the inequality by $zn > 0$, adding $r^2/(2zn)^2$, and rearranging gives

$$\|\delta\|^{2z} - \frac{r}{zn}\|\delta\|^\dagger + \left(\frac{r}{2zn}\right)^2 \leq \frac{b}{zn} + \left(\frac{r}{2zn}\right)^2.$$

Rewriting the previous display yields

$$\left(\|\delta\|^\dagger - \frac{r}{2zn}\right)^2 \leq \frac{b}{zn} + \left(\frac{r}{2zn}\right)^2$$

and

$$\|\delta\|^\dagger \leq \sqrt{\frac{b}{zn} + \left(\frac{r}{2zn}\right)^2} + \frac{r}{2zn}.$$

Finally, using the assumption that $\|\cdot\| \leq \|\cdot\|^\dagger$, we obtain

$$\|\delta\| \leq \sqrt{\frac{b}{zn} + \left(\frac{r}{2zn}\right)^2} + \frac{r}{2zn} \leq \sqrt{\frac{b}{zn}} + \frac{r}{zn},$$

as desired. \blacksquare

APPENDIX B
ADDITIONAL MATERIALS

We finally provide additional theoretical and empirical results.

A. On the Condition of Lemma 4

We have stated in the main part of the paper that the condition in Lemma 4 is a slightly stronger version of restricted strong convexity. Here, we corroborate that statement. We specify the setup of Section III-A a bit further: we (i) assume Gaussian noise ($\mathbf{u} \sim \mathcal{N}[\mathbf{0}, \sigma^2 \mathbf{I}]$), (ii) impose slightly more restrictive assumptions on the design (the irrepresentability condition [4, Assumption 7.3.1]), (iii) assume ℓ_1 -regularization ($\|\cdot\| = \|\cdot\|_\infty$), and (iv) redefine the optimal tuning parameter slightly ($r^* := 4\|X^\top \mathbf{u}\|_\infty$). These additional specifications facilitate the derivations and help us to focus on the main ideas.

Assumption (iii) allows us to use the primal-dual witness approach as detailed in Lederer [4, Section 7.3] to show that $\|\tilde{\beta}_{\mathcal{S}^c}^r\|^\dagger = 0$ for all $r \geq r^*$. Thus, the condition in the lemma simplifies to

$$L(\beta + \nu) - L(\beta) - \langle \nabla L(\beta), \nu \rangle = \|X\nu\|_2^2 \geq zn\|\nu\|_1^2$$

for all $\beta \in \mathbb{R}^p$ and $\nu \in \mathbb{R}^p$ that satisfy $\|\nu_{\mathcal{S}^c}\|_1 \leq 3\|\nu_{\mathcal{S}}\|_1 + b/r$. We now distinguish two cases:

Case 1: $\|\nu_{\mathcal{S}}\|_1 \geq b/r$

Since

$$\begin{aligned} \|\nu\|_1 &\leq \|\nu_{\mathcal{S}}\|_1 + \|\nu_{\mathcal{S}^c}\|_1 \leq \|\nu_{\mathcal{S}}\|_1 + 3\|\nu_{\mathcal{S}}\|_1 + b/r \\ &\leq 5\|\nu_{\mathcal{S}}\|_1 \leq 5\sqrt{|\mathcal{S}|}\|\nu_{\mathcal{S}}\|_2 \leq 5\sqrt{|\mathcal{S}|}\|\nu\|_2, \end{aligned}$$

the condition stated in the lemma becomes (note that using the argument above, we are considering the worst case of our curvature assumption)

$$\|X\nu\|_2^2 \geq 25zn|\mathcal{S}|\|\nu\|_2^2,$$

which equals the usual restricted strong convexity up to a rescaling of the constant z by $25|\mathcal{S}|$ [24, Pages 291ff]. (Whether that rescaling can be avoided or is intrinsic to the problem of connecting statistical and computational bounds would be an interesting topic for further research.)

Case 2: $\|\nu_{\mathcal{S}}\|_1 < b/r$

We find using 1. the assumed decomposability of the ℓ_1 -norm, 2. the ‘‘cone condition’’ for ν , and 3. the assumption $\|\nu_{\mathcal{S}}\|_1 < b/r$ that

$$\begin{aligned} \|\nu\|_1 &= \|\nu_{\mathcal{S}}\|_1 + \|\nu_{\mathcal{S}^c}\|_1 \\ &\leq \|\nu_{\mathcal{S}}\|_1 + 3\|\nu_{\mathcal{S}}\|_1 + b/r \\ &\leq 5b/r. \end{aligned}$$

Now, since $\nu := \tilde{\beta} - \tilde{\beta}^r$ satisfies $\|\nu_{\mathcal{S}^c}\|_1^\dagger \leq 3\|\nu_{\mathcal{S}}\|_1^\dagger + b/r$ according to Lemma 12, we find $\|\tilde{\beta} - \tilde{\beta}^r\|_1 \leq 5b/r$ for any vector $\tilde{\beta} \in \mathbb{R}^p$ that satisfies $\ell(\tilde{\beta}, 2r) \leq \ell(\tilde{\beta}^r, 2r) + b$. Hence, with our choice $b = r^2/(zn)$, we find a suitable computational bound (cf. Lemma 3)

$$d(\tilde{\beta}^r, \tilde{\beta}^r) = \|\tilde{\beta} - \tilde{\beta}^r\|_\infty \leq 5r/(zn) \quad \forall r \in \mathcal{R}$$

without any restrictions altogether.

The two cases combined illustrate that the condition in Lemma 4 is stronger but still comparable to restricted strong convexity. It would be interesting to study questions of optimality in this context, but this is beyond the scope of this paper.

B. Additional Optimization Theory

Our approach requires the construction of a feasible dual point for the approximated estimator $\tilde{\beta}$. In the following, we describe how to find an explicit expression for such a point. Observe that a dual formulation of the primal objective (9) is [25, 41]

$$\begin{aligned} \bar{\nu}^r := \operatorname{argmax}_{\nu \in \mathbb{R}^n} D(\nu, r) &:= -\frac{r^2}{2}\|\nu - \frac{\mathbf{y}}{r}\|_2^2 + \frac{1}{2}\|\mathbf{y}\|_2^2 \\ &\text{subject to } \|X^\top \nu\| \leq 1. \end{aligned}$$

A primal solution of (9) and the dual solution $\bar{\nu}^r$ above are linked by

$$X\tilde{\beta}^r = \mathbf{y} - r\bar{\nu}^r.$$

This suggests choosing as feasible dual point a rescaled version of the residuals. Given a current primal estimate $\tilde{\beta}$, this yields $\tilde{\nu} = s(\mathbf{y} - X\tilde{\beta})$, where s is given by [42]

$$s := \min \left\{ \max \left\{ \frac{-1}{\|X^\top(\mathbf{y} - X\tilde{\beta})\|}, \frac{\mathbf{y}^\top(\mathbf{y} - X\tilde{\beta})}{r\|\mathbf{y} - X\tilde{\beta}\|_2^2} \right\}, \frac{1}{\|X^\top(\mathbf{y} - X\tilde{\beta})\|} \right\}.$$

This choice for the coefficient s ensures that $\tilde{\nu}$ is the closest (in ℓ_2 -norm) point to \mathbf{y}/r in the feasible set $\{\nu \in \mathbb{R}^n : \|X^\top \nu\| \leq 1\}$.

C. Additional Simulations

In this section, we give additional simulation results for the settings of Sections III-A3a and III-B3a.

Table IV contains results for the setting of Section III-A3a with varying sizes M of the tuning parameter set. The results show that all methods are robust with respect to the specific choice of the tuning parameter set.

Table V contains results for the setting of Section III-B3a with varying correlation ρ . The results show that our method also works for correlated data.

Table VI contains results for the setting of Section III-A3a to compare FOS with Chichignoud et al. [7, Algorithm 1] (we call it AV-test), which corresponds to running FOS with b close to zero (we set $b = 1e - 7$). The results suggest that FOS is much faster and more accurate than AV-test.

Table VII contains results for the setting of Section III-B3a to compare log-FOS with Li and Lederer [11] (we call it LI), which corresponds to running log-FOS with b close to zero (we set again $b = 1e - 7$). The results suggest that log-FOS is much faster than LI in all settings and similarly accurate.

Tables VIII and IX contain results for the setting of Section III-A3a with varying constants z and c , respectively. The

results show that changing z and c has minor impact on our results.

Tables X and XI contain results for the setting of Section III-B3a with varying constants z and c_{\log} , respectively. The results show that changing z and c_{\log} has minor impact on our results.

ACKNOWLEDGMENT

We thank Haim Bar for the insightful comments on a draft version of this manuscript. We also thank the associate editor and the reviewers for their insightful comments. The authors MT and JL acknowledge funding from the Deutsche Forschungsgemeinschaft (DFG) under project number 265592081.

REFERENCES

- [1] R. Tibshirani, "Regression shrinkage and selection via the lasso," *J. R. Stat. Soc. Ser. B Stat. Methodol.*, vol. 58, no. 1, pp. 267–288, 1996.
- [2] S. Bakin, "Adaptive regression and model selection in data mining problems," 1999.
- [3] M. Yuan and Y. Lin, "Model selection and estimation in regression with grouped variables," *J. Roy. Statist. Soc. Ser. B.*, vol. 68, no. 1, pp. 49–67, 2006.
- [4] J. Lederer, *Fundamentals of high-dimensional statistics— with exercises and R labs*. Springer Series in Statistics, 2022.
- [5] P. Bühlmann and S. van de Geer, *Statistics for high-dimensional data: methods, theory and applications*, ser. Springer Ser. Statist., 2011.
- [6] M. Wainwright, *High-dimensional statistics: a non-asymptotic viewpoint*. Cambridge Univ. Press, 2019, vol. 48.
- [7] M. Chichignoud, J. Lederer, and M. Wainwright, "A practical scheme and fast algorithm to tune the lasso with optimality guarantees," *J. Mach. Learn. Res.*, vol. 17, no. 1, pp. 8162–8188, 2016.
- [8] D. Chételat, J. Lederer, and J. Salmon, "Optimal two-step prediction in regression," *Electron. J. Stat.*, vol. 11, no. 1, pp. 2519–2546, 2017.
- [9] M. Laszkiewicz, A. Fischer, and J. Lederer, "Thresholded adaptive validation: Tuning the graphical lasso for graph recovery," in *International Conference on Artificial Intelligence and Statistics*. PMLR, 2021, pp. 1864–1872.
- [10] S. Huang, Y. Düren, K. Hellton, and J. Lederer, "Tuning parameter calibration for personalized prediction in medicine," *Electron. J. Stat.*, vol. 15, no. 2, pp. 5310–5332, 2021.
- [11] W. Li and J. Lederer, "Tuning parameter calibration for ℓ_1 -regularized logistic regression," *J. Statist. Plann. Inference*, vol. 202, pp. 80–98, 2019.
- [12] R. Judson, B. Salisbury, J. Schneider, A. Windemuth, and J. Stephens, "How many SNPs does a genome-wide haplotype map require?" *Pharmacogenomics*, vol. 3, no. 3, pp. 379–391, 2002.
- [13] F. Bunea, J. Lederer, and Y. She, "The group square-root lasso: Theoretical properties and fast algorithms," *IEEE Trans. Inform. Theory*, vol. 60, no. 2, pp. 1313–1325, 2013.
- [14] J. Friedman, T. Hastie, and R. Tibshirani, "Regularization paths for generalized linear models via coordinate descent," *J. Stat. Softw.*, vol. 33, no. 1, pp. 1–22, 2010.
- [15] M. Osborne, B. Presnell, and B. Turlach, "On the lasso and its dual," *J. Comput. Graph. Statist.*, vol. 9, no. 2, pp. 319–337, 2000.
- [16] Y. Hu, C. Li, K. Meng, J. Qin, and X. Yang, "Group sparse optimization via $\ell_{p,q}$ regularization," *J. Mach. Learn. Res.*, vol. 18, no. 1, pp. 960–1011, 2017.
- [17] S. Negahban, P. Ravikumar, M. Wainwright, and B. Yu, "A unified framework for high-dimensional analysis of M -estimators with decomposable regularizers," *Statist. Sci.*, vol. 27, no. 4, pp. 538–557, 2012.
- [18] M. Wainwright, "Structured regularizers for high-dimensional problems: statistical and computational issues," *Annu. Rev. Stat. Appl.*, vol. 1, pp. 233–253, 2014.
- [19] V. Koltchinskii, "Sparsity in penalized empirical risk minimization," *Ann. Inst. Henri Poincaré Probab. Stat.*, vol. 45, no. 1, pp. 7–57, 2009.
- [20] S. van de Geer and P. Bühlmann, "On the conditions used to prove oracle results for the lasso," *Electron. J. Stat.*, vol. 3, pp. 1360–1392, 2009.
- [21] J. Lederer and M. Vogt, "Estimating the lasso's effective noise," *JMLR*, vol. 22, no. 276, pp. 1–32, 2021.
- [22] J. Lederer, L. Yu, and I. Gaynanova, "Oracle inequalities for high-dimensional prediction," *Bernoulli*, vol. 25, no. 2, pp. 1225–1255, 2019.
- [23] A. Dalalyan, M. Hebiri, and J. Lederer, "On the prediction performance of the lasso," *Bernoulli*, vol. 23, no. 1, pp. 552–581, 2017.
- [24] T. Hastie, R. Tibshirani, and M. Wainwright, *Statistical learning with sparsity: the lasso and generalizations*. CRC press, 2015.
- [25] J. Borwein and A. Lewis, *Convex analysis and nonlinear optimization: theory and examples*. Springer Science & Business Media, 2010.
- [26] A. Beck and M. Teboulle, "A fast iterative shrinkage-thresholding algorithm for linear inverse problems," *SIAM J. Imaging Sci.*, vol. 2, no. 1, pp. 183–202, 2009.
- [27] J. Fan and R. Li, "Variable selection via nonconcave penalized likelihood and its oracle properties," *J. Amer. Statist. Assoc.*, vol. 96, no. 456, pp. 1348–1360, 2001.
- [28] C. Zhang, "Nearly unbiased variable selection under minimax concave penalty," *Ann. Statist.*, vol. 38, no. 2, pp. 894–942, 2010.
- [29] F. Bach, R. Jenatton, J. Mairal, and G. Obozinski, "Convex optimization with sparsity-inducing norms," in *Optimization for Machine Learning*. MIT Press, 2011.
- [30] H. Zhou, A. Armagan, and D. Dunson, "Path following and empirical bayes model selection for sparse regression," *arXiv:1201.3528*, 2012.
- [31] S. Kogan, D. Levin, B. Routledge, J. Sagi, and N. Smith, "Predicting risk from financial reports with regression," in *HLT-NAACL*, 2009, pp. 272–280.
- [32] I. Guyon, C. Aliferis, G. Cooper, A. Elisseeff, J. Pellet, P. Spirtes, and A. Statnikov, "Design and analysis of the

TABLE IV

THE AVERAGE RUN TIMES (IN SECONDS) AND AVERAGE HAMMING DISTANCES IN THESE SETTINGS ILLUSTRATE THE LIMITED INFLUENCE OF THE SPECIFIC CHOICE OF THE TUNING PARAMETER SET

$n = 500, p = 500, s = 10, \rho = 0.3$					
Method	$M = 500$		$M = 1000$		Hamming distance
	Timing	Hamming distance	Timing	Hamming distance	
lassoCV _{SPAMS}	313.34 ± 21.93	50.80 ± 16.07	578.00 ± 43.15	50.60 ± 16.20	
SCAD	74.91 ± 13.56	55.00 ± 30.98	173.19 ± 50.32	56.20 ± 15.35	
MCP	77.36 ± 13.42	54.80 ± 38.15	177.97 ± 51.46	49.40 ± 6.65	
FOS	0.21 ± 0.09	1.00 ± 3.16	0.53 ± 0.14	1.30 ± 4.11	

$n = 500, p = 500, s = 10, \rho = 0.3$					
Method	$M = 2000$		$M = 4000$		Hamming distance
	Timing	Hamming distance	Timing	Hamming distance	
lassoCV _{SPAMS}	NA	NA	NA	NA	
SCAD	324.21 ± 107.43	67.00 ± 13.29	NA	NA	
MCP	361.54 ± 121.90	57.50 ± 5.74	NA	NA	
FOS	1.91 ± 0.52	1.30 ± 4.11	13.88 ± 3.85	1.50 ± 4.74	

TABLE V

THE AVERAGE RUN TIMES (IN SECONDS) AND AVERAGE HAMMING DISTANCES IN THESE SETTINGS ILLUSTRATE THAT LOG-FOS PERFORMS WELL ACROSS A WIDE SPECTRUM OF CORRELATIONS

$n = 200, p = 500, s = 15$					
Method	$\rho = 0.0$		$\rho = 0.25$		Hamming distance
	Timing	Hamming distance	Timing	Hamming distance	
log-lassoCV _{SPAMS}	19.97 ± 0.76	11.50 ± 5.44	22.94 ± 0.70	14.60 ± 3.94	
log-FOS	0.89 ± 0.10	9.30 ± 4.19	0.86 ± 0.05	10.60 ± 6.22	

$n = 200, p = 500, s = 15$					
Method	$\rho = 0.5$		$\rho = 0.75$		Hamming distance
	Timing	Hamming distance	Timing	Hamming distance	
log-lassoCV _{SPAMS}	24.61 ± 2.23	15.40 ± 2.11	24.24 ± 3.10	16.70 ± 2.94	
log-FOS	0.85 ± 0.07	10.90 ± 2.76	0.85 ± 0.07	14.70 ± 2.35	

$n = 1000, p = 5000, s = 15$					
Method	$\rho = 0.0$		$\rho = 0.25$		Hamming distance
	Timing	Hamming distance	Timing	Hamming distance	
log-lassoCV _{SPAMS}	NA	NA	NA	NA	
log-FOS	25.95 ± 3.93	7.20 ± 3.70	30.50 ± 2.99	6.80 ± 2.14	

$n = 1000, p = 5000, s = 15$					
Method	$\rho = 0.5$		$\rho = 0.75$		Hamming distance
	Timing	Hamming distance	Timing	Hamming distance	
log-lassoCV _{SPAMS}	NA	NA	NA	NA	
log-FOS	41.84 ± 4.67	8.30 ± 1.94	33.89 ± 1.64	12.40 ± 2.54	

TABLE VI

AVERAGE RUN TIMES (IN SECONDS), HAMMING DISTANCES, AND ESTIMATION ERRORS FOR AV-TEST AND FOS WITH $M = 100$. THE RESULTS ILLUSTRATE THAT FOS IS BOTH FASTER AND MORE ACCURATE THAN AV-TEST

Method	$n = 500, p = 1000$			$n = 5000, p = 10000$		
	Timing	Hamming distance	Estimation error	Timing	Hamming distance	Estimation error
AV-test	0.35 ± 0.13	2.30 ± 0.82	0.39 ± 0.02	63.28 ± 11.20	0.60 ± 0.84	0.31 ± 0.02
FOS	0.08 ± 0.07	1.00 ± 2.82	0.19 ± 0.04	5.80 ± 3.06	0.00 ± 0.00	0.10 ± 0.02

causation and prediction challenge,” in *WCCI Causation and Prediction Challenge*, 2008, pp. 1–33.

- [33] N. Meinshausen and P. Bühlmann, “High-dimensional graphs and variable selection with the lasso,” *Ann. Statist.*, vol. 34, no. 3, pp. 1436–1462, 2006.
- [34] A. Statnikov, S. Ma, M. Henaff, N. Lytkin, E. Efstathiadis, E. Peskin, and C. Aliferis, “Ultra-scalable and efficient methods for hybrid observational and experimental local causal pathway discovery,” *J. Mach. Learn. Res.*, vol. 16, no. 1, pp. 3219–3267, 2015.
- [35] X. Ma, Z. Wang, P. Ryan, S. Isakoff, A. Barmettler, A. Fuller, B. Muir, G. Mohapatra, R. Salunga, J. Tuggle, and Y. Tran, “A two-gene expression ratio predicts clinical outcome in breast cancer patients treated with tamoxifen,” *Cancer cell*, vol. 5, no. 6, pp. 607–616, 2004.
- [36] A. Subramanian, P. Tamayo, V. Mootha, S. Mukherjee, B. Ebert, M. Gillette, A. Paulovich, S. Pomeroy, T. Golub, E. Lander, and J. Mesirov, “Gene set enrichment analysis: a knowledge-based approach for interpreting genome-wide expression profiles,” *Proc. Nat. Acad. Sci. India Sect. A*, vol. 102, no. 43, pp. 15 545–15 550, 2005.
- [37] P. Zhao and B. Yu, “On model selection consistency of lasso,” *J. Mach. Learn. Res.*, vol. 7, pp. 2541–2563, 2006.
- [38] S. Mian, S. Ugurel, E. Parkinson, I. Schlenzka, I. Dryden, L. Lancashire, G. Ball, C. Creaser, R. Rees, and

TABLE VII
AVERAGE RUN TIMES (IN SECONDS), HAMMING DISTANCES, AND ESTIMATION ERRORS FOR LI AND LOG-FOS WITH $M = 500$. THE RESULTS ILLUSTRATE THAT LOG-FOS IS FASTER AND SIMILARLY ACCURATE

$n = 200, p = 200, s = 8$						
Method	$\rho = 0.25$			$\rho = 0.5$		
	Timing	Hamming distance	Estimation error	Timing	Hamming distance	Estimation error
LI	2.09 ± 0.33	2.90 ± 1.19	2.25 ± 0.60	2.80 ± 0.37	5.3 ± 1.63	2.50 ± 0.68
log-FOS	0.36 ± 0.06	3.10 ± 1.79	2.04 ± 0.59	0.58 ± 0.03	5.6 ± 2.11	2.35 ± 0.69
$n = 200, p = 500, s = 8$						
Method	$\rho = 0.25$			$\rho = 0.5$		
	Timing	Hamming distance	Estimation error	Timing	Hamming distance	Estimation error
LI	3.89 ± 0.46	3.6 ± 1.34	2.57 ± 0.17	6.43 ± 0.89	5.5 ± 1.58	2.73 ± 0.34
log-FOS	1.22 ± 0.07	4.4 ± 1.95	2.36 ± 0.16	1.09 ± 0.04	8.6 ± 3.83	2.56 ± 0.36
$n = 1000, p = 5000, s = 8$						
Method	$\rho = 0.25$			$\rho = 0.5$		
	Timing	Hamming distance	Estimation error	Timing	Hamming distance	Estimation error
LI	142.50 ± 53.98	7.9 ± 0.31	2.93 ± 0.58	314.29 ± 130.60	7.0 ± 1.05	2.98 ± 0.58
log-FOS	33.64 ± 4.69	4.7 ± 1.33	2.48 ± 0.58	25.95 ± 4.23	3.8 ± 1.68	2.54 ± 0.57

TABLE VIII
AVERAGE RUN TIMES (IN SECONDS), HAMMING DISTANCES, AND ESTIMATION ERRORS FOR FOS, WITH $M = 100$. THE RESULTS ILLUSTRATE THE LIMITED INFLUENCE OF THE SPECIFIC CHOICE OF z

$n = 500, p = 1000, c = 2$			
Method	Timing	Hamming distance	Estimation error
FOS($z = 1$)	0.12 ± 0.08	1.0 ± 2.82	0.19 ± 0.04
FOS($z = 2$)	0.09 ± 0.05	0.6 ± 1.57	0.19 ± 0.04
FOS($z = 4$)	0.09 ± 0.02	0.6 ± 1.57	0.20 ± 0.04

TABLE IX
AVERAGE RUN TIMES (IN SECONDS), HAMMING DISTANCES, AND ESTIMATION ERRORS FOR FOS, WITH $M = 100$. THE RESULTS ILLUSTRATE THE LIMITED INFLUENCE OF THE SPECIFIC CHOICE OF c

$n = 500, p = 1000, z = 1$			
Method	Timing	Hamming distance	Estimation error
FOS($c = 2$)	0.12 ± 0.08	1.0 ± 2.82	0.19 ± 0.04
FOS($c = 3$)	0.04 ± 0.01	0.3 ± 0.67	0.31 ± 0.03
FOS($c = 4$)	0.03 ± 0.01	2.4 ± 1.26	0.42 ± 0.04

TABLE X
AVERAGE RUN TIMES (IN SECONDS), HAMMING DISTANCES, AND ESTIMATION ERRORS FOR LOG-FOS, WITH $M = 500$. THE RESULTS ILLUSTRATE THE LIMITED INFLUENCE OF THE SPECIFIC CHOICE OF z

$n = 200, p = 200, \rho = 0.25, c_{\log} = 6$			
Method	Timing	Hamming distance	Estimation error
log-FOS($z = 1$)	0.36 ± 0.06	3.1 ± 1.79	2.04 ± 0.59
log-FOS($z = 2$)	0.78 ± 0.06	4.4 ± 1.95	2.36 ± 0.16
log-FOS($z = 4$)	0.73 ± 0.02	4.4 ± 1.95	2.36 ± 0.16

TABLE XI
AVERAGE RUN TIMES (IN SECONDS), HAMMING DISTANCES, AND ESTIMATION ERRORS FOR LOG-FOS, WITH $M = 500$. THE RESULTS ILLUSTRATE THE LIMITED INFLUENCE OF THE SPECIFIC CHOICE OF c_{\log}

$n = 200, p = 200, \rho = 0.25, z = 1$			
Method	Timing	Hamming distance	Estimation error
log-FOS($c_{\log} = 6$)	0.36 ± 0.06	3.1 ± 1.79	2.04 ± 0.59
log-FOS($c_{\log} = 8$)	0.33 ± 0.05	4.0 ± 1.76	1.95 ± 0.59
log-FOS($c_{\log} = 4$)	0.32 ± 0.02	2.9 ± 0.99	2.17 ± 0.60

- D. Schadendorf, "Serum proteomic fingerprinting discriminates between clinical stages and predicts disease progression in melanoma patients," *J. Clin. Oncol.*, vol. 23, no. 22, pp. 5088–5093, 2005.
- [39] J. Lederer and C. Müller, "Don't fall for tuning parameters: tuning-free variable selection in high dimensions with the TREX," in *Twenty-Ninth AAAI Conference on Artificial Intelligence*, 2015.
- [40] F. Bach, R. Jenatton, J. Mairal, and G. Obozinski, "Optimization with sparsity-inducing penalties," *arXiv:1108.0775.*, 2011.
- [41] E. Ndiaye, O. Fercoq, A. Gramfort, and J. Salmon, "Gap safe screening rules for sparse-group lasso," in *NIPS*, 2016, pp. 388–396.
- [42] L. Ghaoui, V. Viallon, and T. Rabbani, "Safe feature elimination for the lasso and sparse supervised learning problems," *arXiv:1009.4219.*, 2010.

Mahsa Taheri received her Master's degree in Artificial Intelligence from IUT, Iran, in 2017. She is currently pursuing a Ph.D. degree in Mathematical Statistics at the Ruhr-University Bochum. Her research interests include statistics and theoretical machine learning, specifically, theory of deep learning.

Néhémy Lim is a Data Engineering consultant at Business and Decision. His research interests include high-dimensional statistics, time series forecasting, and machine learning with applications in biology. He received the Ph.D. degree in Computer Science from Université d'Évry-Val-d'Essonne in 2015. He was a postdoctoral research associate at the University of Washington from 2015 to 2017 and a visiting assistant professor at the University of Connecticut from 2017 to 2020.

Johannes Lederer is Professor of Mathematical Statistics at the Ruhr-University Bochum. His educational training spans physics, mathematics, and statistics. After receiving a MSc in Physics, he started his Doctor of Sciences under the supervision of Sara van de Geer and Peter Bühlmann at ETH Zürich in December 2009 and completed the degree in December 2012. After that, he was a post-doctoral researcher hosted by Martin Wainwright at UC Berkeley, until he accepted the position as the Jacob Wolfowitz Visiting Assistant Professor in the Department of Statistical Science at Cornell University in August 2013. In September 2015, he joined the University of Washington as Tenure-Track Assistant Professor of Statistics and Adjunct Assistant Professor of Biostatistics at the University of Washington. In December 2017, Johannes was appointed in Bochum. Johannes is also Affiliate Faculty at the University of Washington and Associate Editor of the Canadian Journal of Statistics.